BASIN-RING SPACING ON THE MOON, MERCURY, AND MARS

RICHARD. J. PIKE
U.S. Geological Survey, Menlo Park, California, U.S.A.
and
PAUL D. SPUDIS
U.S. Geological Survey, Flagstaff, Arizona, U.S.A.

(Received 26 November, 1986)

Abstract. Radial spacing between concentric rings of impact basins that lack central peaks is statistically similar and nonrandom on the Moon, Mercury, and Mars, both inside and outside the main ring. One spacing interval, $(2.0 \pm 0.3)^{0.5}$D, or an integer multiple of it, dominates most basin rings. Three analytical approaches yield similar results from 296 remapped or newly mapped rings of 67 multi-ringed basins: least-squares of rank-grouped rings, least-squares of rank and ring diameter for each basin, and averaged ratios of adjacent rings. Analysis of 106 rings of 53 two-ring basins by the first and third methods yields an integer multiple $(2 \times)$ of $2.0^{0.5}$D. There are two exceptions: (1) Rings adjacent to the main ring of multi-ring basins are consistently spaced at a slightly, but significantly, larger interval, $(2.1 \pm 0.3)^{0.5}$D; (2) The 88 rings of 44 protobasins (large peak-plus-inner-ring craters) are spaced at an entirely different interval $(3.3 \pm 0.6)^{0.5}$D.

The statistically constant and target-invariant spacing of so many rings suggests that this characteristic may constrain formational models of impact basins on the terrestrial planets. The key elements of such a constraint include: (1) ring positions may not have been located by the same process(es) that formed ring topography; (2) ring location and emplacement of ring topography need not be coeval; (3) ring location, but not necessarily the mode of ring emplacement, reflects one process that operated at the time of impact; and (4) the process yields similarly-disposed topographic features that are spatially discrete at $2^{0.5}$D intervals, or some multiple, rather than continuous. These four elements suggest that some type of wave mechanism dominates the location, but not necessarily the formation, of basin rings. The waves may be standing, rather than travelling. The ring topography itself may be emplaced at impact by this and/or other mechanisms and may reflect additional, including post-impact, influences.

1. Introduction

The origin of large concentric-ringed impact structures, or 'basins', remains an outstanding unsolved problem in planetology. Radial spacing of the ring diameters, D, may provide quantitative photogeologic constraints on geophysical models proposed to explain basins. In this paper, we try to ascertain whether or not the oft-cited $2^{0.5}$D spacing interval between rings (Fielder, 1963) is valid for terrestrial planets, and hence worthy of consideration as a key ingredient in basin hypotheses.

Impact basins are ubiquitous on solid planets and large satellites throughout the solar system (Hartmann, 1981; Moore *et al.*, 1984). Large multiple-ringed basins (Figures 1–3) are so common on the Moon, Mars, and Mercury that they constitute the broad-scale structural framework of the upper crust on these bodies (Wilhelms and McCauley, 1971; Schultz, 1984; Spudis and Strobell, 1984). It has been suggested, ever since basin ring diameters were first measured on the Moon (Hartmann and Kuiper, 1962; Hartmann and Wood, 1971; Howard *et al.*, 1974), that

Earth, Moon, and Planets **39** (1987) 129–194.

radial spacing of basin rings on the three planets is not random (Wood and Head, 1976).

1.1. The problem

Opinion on the regularity of ring spacing, its relevance to basin origin, and even existence of many of the rings remains polarized. For example, contrast '... reality of the $2^{0.5}$ relation has been and remains obvious ... no one has ever doubted that.' (C. A. Wood, personal communication, dated 1/20/1986) with 'I am unconvinced ... that more than 2 or 3 rings surround basins on the Moon, Mars, or Mercury'. and '... the putative $2^{0.5}$ ring spacing ...' (H. J. Melosh, personal communication, 11/18/85). The 1980 conference on multi-ring basins (Schultz and Merrill, 1981) did not even address, much less resolve these key issues.

The spacing of basin rings has been cited as evidence for strongly contrasting explanations to the problem of basin formation. A high degree of spatial orderliness, by which successively larger rings increase in D by a nearly constant multiplier, or spacing increment, invariably $2^{0.5}$D or 2D, is claimed by some to support certain physical models for ring origin (Baldwin, 1963, 1974; Fielder, 1963; Van Dorn, 1968, 1969; Chadderton *et al.*, 1969; Floran and Dence, 1976; Murray, 1980; Pike, 1981; Pike and Spudis, 1984a, b). However, the spacing of rings is not everywhere as systematic and clear-cut as at, say, Orientale on the Moon (Howard *et al.*, 1974; Wilhelms, 1980a; Pike, 1985). Numerical values for the spacing increment and the degree of certainty with which they describe basin rings are both controversial. Accordingly, a low or moderate degree of spatial orderliness among rings also has been invoked in devising other, markedly different, hypotheses to explain ring and basin formation (Head, 1977a; Wilhelms *et al.*, 1977; Hodges and Wilhelms, 1978; Melosh and McKinnon, 1978; Solomon and Head, 1980; McKinnon and Melosh, 1980; Croft, 1981a). We return to differences among these contending models later.

Past numerical treatment of ring spacing has been casual: typically by graphs, histograms, and lists of ratios. This had resulted partly from the small data set, largely from the Moon (e.g., Wilhelms *et al.*, 1977). Past work also failed to recognize major size-dependent differences in ring geometry between some two- and multi-ring basins (Pike, 1983). Finally, earlier work emphasized the central tendency of ring ratios at certain values but ignored their dispersion. Thus, the non-randomness of ring spacing has never been tested formally, and it has been difficult to judge the reality and strength of any spacing 'law'.

1.2. Approach and scope

This paper reexamines the problem of basin ring spacing using abundant new observations and a more rigorous analysis. Recently, the data set has been greatly augmented by the discovery of many old and/or degraded multi-ring basins on both Mars (Schultz and Glicken, 1979) and Mercury (Spudis, 1984). To address the uncertainties of basin-ring spacing we have (1) mapped or remapped almost 500 rings on the Moon, Mercury, and Mars; and (2) analyzed their diameters by three statistical

approaches: rank-grouped correlation, size/rank correlation for individual basins, and ring ratios. Formal statistical tests are carried out in all three analyses.

We have limited this investigation to the three planets that provide the most statistically adequate sample. Moreover, the Moon, Mercury, and Mars may differ sufficiently in crustal properties, thermal history, and to a lesser extent gravity (Carr *et al.*, 1984), that planet-specific differences in ring spacing for terrestrial bodies should become evident. Brief summaries of some results have been published (Pike and Spudis, 1984a, b). What appear to be related types of basins also occur on Earth, Ganymede, Rhea, Tethys, and perhaps Callisto, but they are much less common, and the ring-spacing statistics are commensurately less robust. Preliminary formal study of their ring geometry has been reported elsewhere; first results on spacing intervals are consistent with those found here (Pike, 1985).

Current basin nomenclature is unsatisfactory: (1) The term 'peak-ring basin' (PRB; e.g. Wood and Head, 1976) for two-ring structures (Figure 4; Hartmann and Kuiper, 1962; Stuart-Alexander and Howard, 1970) implies the inner ring is analogous genetically to the central peak found in craters – a contention not yet demonstrated. (2) 'Central-peak basins' (CPB) morphologically resemble large craters more than basins (Figure 5; Stuart-Alexander and Howard, 1970; Hartmann and Wood, 1971; Baldwin, 1974). Moreover, as we show here (see also Pike, 1983), the inner ring is systematically smaller than it is in two-ring basins, so much so that the two cannot be included in the same analysis. In this paper, we refer to a 'two-ring basin' as such and adopt the expressly transitional term 'protobasin' (Pike, 1983) for the large peak-plus-ring structures that are neither strictly craters nor basins. We retain the excellent term 'multi-ring basin' for structures with three or more rings (Figures 1–3; Hartmann and Wood, 1971).

This paper examines all three classes of basins. Two-ring basins and protobasins are particularly important because (1) they are related genetically to the larger, multi-ring, basins and their attributes surely bear on the problem of spacing between multiple rings (Pike, 1982, 1983, 1985), and (2) the existence and dimensions of their rings are more certain and widely accepted than are those of some of the multi-ring basins listed here.

2. Recognizing and Mapping Basin Rings

Concentric geologic structures and the impact process were first linked causally on Earth (Boon and Albritton, 1936). Only later were multi-ring and then two-ring basins recognized on the Moon (Figure 1) as large, concentric, and circular patterns that appeared to be loci of the dark, low-lying (and presumably volcanic) maria (Dietz, 1946; Baldwin, 1949, 1963; Hartmann and Kuiper, 1962). The process by which these broad-scale, fundamental structures were interpreted from the confusing detail of planetary surfaces has been described by Hartmann (1981). Progressively more degraded basins were recognized on the Moon as its geologic mapping continued. Interpretation has matured to the point where ringed lunar structures that

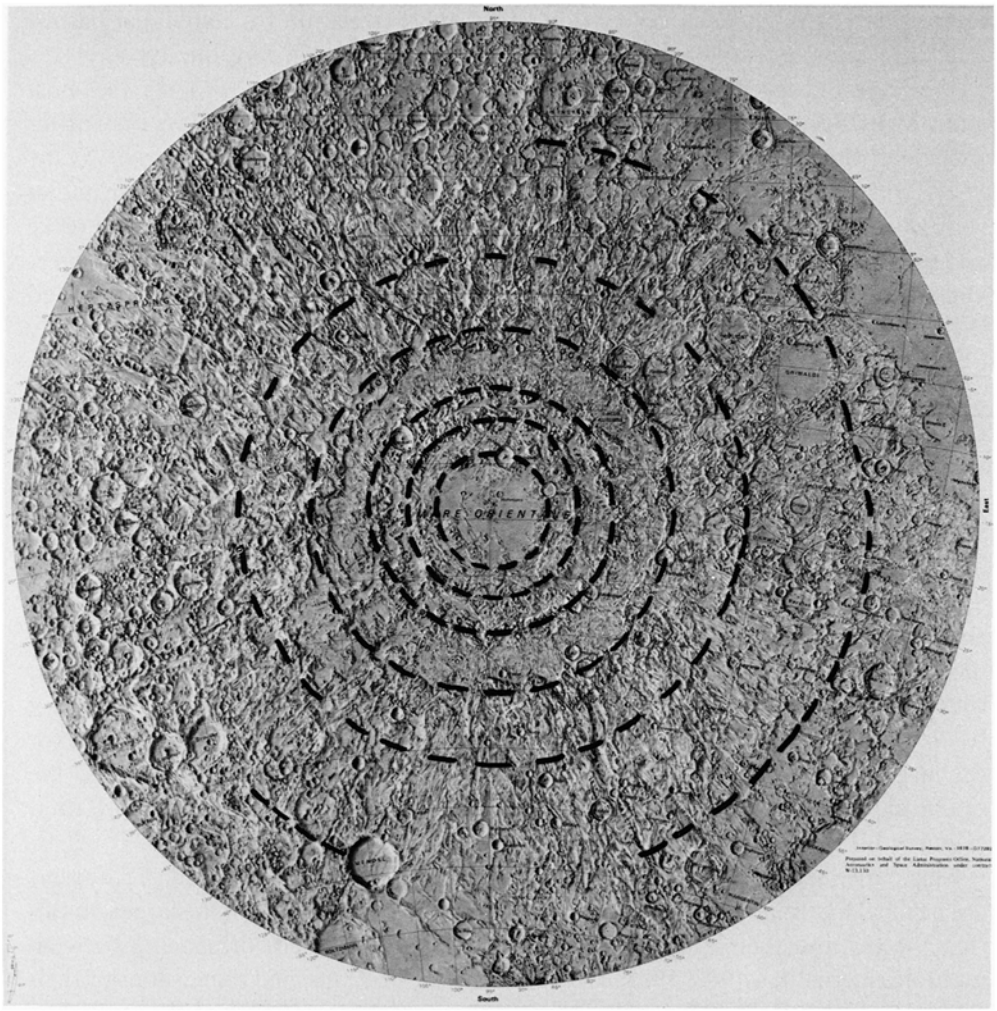

Fig. 1a. Six-ring interpretation of the Orientale basin, Moon, after Hartmann and Kuiper (1962). Outermost ring, about 1900 km in diameter (Table I), depicted only where photogeologic elements can be recognized. Stereographic-projection base map by U.S. Geological Survey.

are all but completely obliterated (e.g. the two- or three-ringed Al-Khwarizmi-King basin, not included here) have been recognized and mapped (El-Baz, 1972; Wilhelms and El-Baz, 1977). The total of 'known' lunar basins now stands at 30 to 40 (Wilhelms, 1980b, 1984), and a dozen more are 'possible' (Wilhelms, 1984).

It was helpful that the first extraterrestrial body studied geologically, the Moon, has many basins in various degrees of degradation, for it was the experience of lunar mapping that enabled similar structures to be quickly identified on more distant planets (Figures 2, 3; e.g. Wilhelms, 1973; Murray *et al.*, 1974). Recently, more than

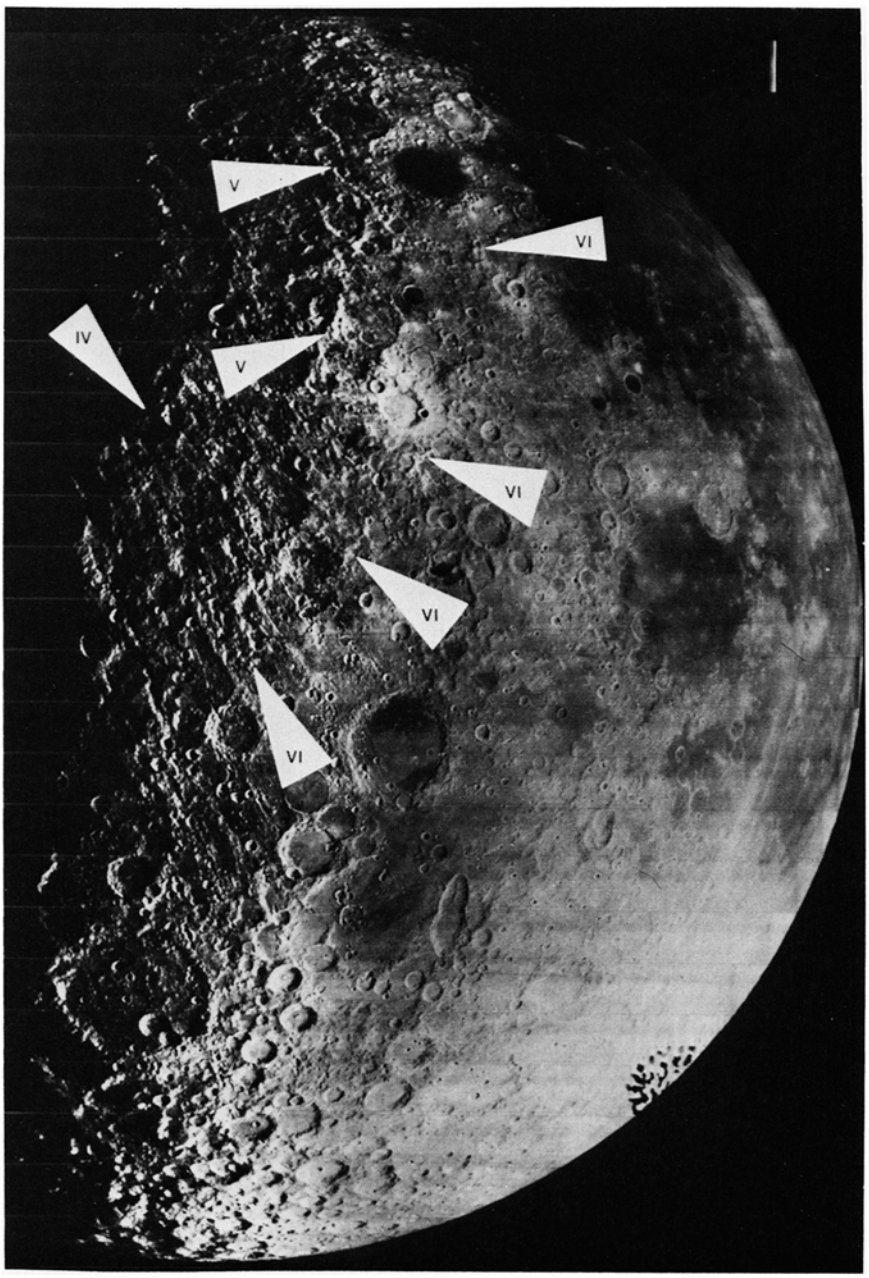

Fig. 1b. Eastern part of the Orientale basin region, showing evidence for its two most cryptic rings (see also Hartmann and Kuiper, (1962, Plate 12.42)). Main ring (Cordillera, rank IV) is 930 km in diameter (Table I). Ring just exterior to Cordillera indicated as rank V. Outermost Orientale ring (rank VI) delineated by massifs, arcuate topographic highs, and scarp-like features. North at top; portion of Lunar Orbiter IV image 167M.

20 old multi-ring basins have been discovered on both Mars (Schultz and Glicken, 1979; Schultz *et al.*, 1982; Stam *et al.*, 1984) and Mercury (Spudis, 1984; Spudis and Prosser, 1984). Many of these features are as highly degraded as the most obscure lunar basin. Recognition and delimitation of old multi-ring basins, specifically deciding on ring positions and dimensions, require detailed study and terrain mapping of the sort carried out by Schultz and Glicken (1979) and Schultz *et al.* (1982). The techniques are illustrated here by three large basins, on the Moon, Mercury, and Mars, whose preservation states range from obvious to cryptic. The following description of the mapping methods will also illustrate some of the uncertainties inherent in the data for multi-ring basins (Table I). Two-ring structures, a much simpler case (Table II), are discussed separately in Section 2.5.

2.1. ORIENTALE BASIN, MOON

Orientale is the youngest and freshest multi-ring basin on the Moon (Figure 1). A concentric, multi-ring form for this feature was first described in detail by Hartmann and Kuiper (1962) from rectified Earth-based telescopic photographs. Following acquisition of the Zond and Lunar Orbiter images, the geology of the basin was described repeatedly (e.g. McCauley, 1968, 1977; Hartmann and Wood, 1971; Moore *et al.*, 1974; Head, 1974; Schultz, 1976). Figure 1a shows our 6-ring interpretation of the ringed structure of Orientale. It is based largely on that of Hartmann and Kuiper (1962).

Locations and dimensions of basin rings within the 930 km-diameter Cordillera scarp, the main ring (initially the 'Eichstadt' ring), are well accepted, but rings exterior to it are less so (Table I). The three interior rings are defined clearly by concentric alignments of massifs and scarps. Some irregularities are evident in the circular patterns, but most students of impact basins agree on diameters of the innermost four rings (cf. Head, 1974; Wilhelms *et al.*, 1977; Croft, 1979; Wilhelms, 1984). The smallest and best exposed ring outside the Cordillera scarp (the 'Rocca' ring) was recognized by Hartmann and Kuiper (1962) and is listed by Croft (1979). Some later work (Head, 1974; Moore *et al.*, 1974; Hodges and Wilhelms, 1978; Croft, 1981b; and Wilhelms, 1984) has not addressed the presence of this ring, but the evidence for it (Figure 1b; Hartmann and Kuiper, 1962, Plate 12.42) is compelling.

We have identified components of a sixth, discontinuous, Orientale ring beyond the 'Rocca' ring. Although detected by Gerard Kuiper in Hartmann and Kuiper (1962, Plate 12.42) and mentioned in the text, it was not listed explicitly in their summary table. Our evidence for a sixth ring consists of discontinuous massif elements (Figure 1b), undulating and concentric topographic highs that are buried by Orientale ejecta at about $-47°$, 114° W (near crater Mendel), and scarp-like terrain. The massif elements shown in Figure 1b do not appear to be associated with other, pre-Orientale features: they are not central peaks or parts of other basin rims.

The contrast in prominence between the crisp inner and vague outer rings of Orientale, the least modified lunar basin, has prompted the generalization (e.g.,

TABLE I

Ring diameters, ranks, and weights for 67 multi-ring basins[a]

Basin[b]	Center Coordinates (deg)	Mean observed ring diameters (km)[c, d]								
		"B"	"A"	I	II	III	IV	V	VI	VII
					Moon					
Orientale	−19, 95 W	–	–	320	480	620	930	1300	(1900)	–
Imbrium	+35, 17 W	–	–	–	550	790	1160	(1700)	(2250)	[3200]
Nectaris	−16, 34 E	–	240	–	400	620	860	(1320)	–	–
Moscoviense	+26, 148 E	–	–	[140]	220	[300]	420	(630)	–	–
Mendel-Rydberg	−50, 94 W	–	–	–	[200]	(300)	420	630	–	–
Hertzsprung	+02, 128 W	–	[150]	–	255	(380)	570	–	–	–
Humorum	−24, 39 W	–	–	–	[210]	[340]	425	(570)	800	(*1195*)
Smythii	−02, 87 E	–	–	(260)	370	540	740	[1130]	–	–
Crisium	+18, 59 E	–	–	–	–	360	540	740	1080	(1600)
Grimaldi	−06, 68 W	–	–	–	230	300	440	–	–	–
Humboldtianum	+59, 82 E	–	–	(250)	340	460	650	1050	(1350)	
Coulomb-Sarton	+52, 123 W	–	–	(160)	(250)	–	(440)	(670)	–	–
Serenitatis South	+26, 18 E	–	–	–	410	620	920	1300	(1880)	–
Korolev	−04, 158 W	–	–	–	220	–	440	590	[*810*]	–
Ingenii	−43, 165 E	–	–	–	[165]	–	315	450	[*660*]	–
Apollo	−36, 151 W	–	–	–	240	–	480	(720)	–	–
Balmer	−15, 70 E	–	–	–	–	260	400	(580)	–	–
Keeler-Heaviside	−10, 162 E	–	–	–	–	(325)	500	750	[1000]	–

Table I (continued)

Mercury

Basin[b]	Center Coordinates (deg)	Mean observed ring diameters (km)[c, d]								
		"B"	"A"	I	II	III	IV	V	VI	VII
Borealis	+73, 53 W	–	–	–	(860)	–	1530	[2230]	–	–
Gluck-Holbein	+35, 19 W	–	–	–	(240)	–	500	–	(950)	–
Derzhavin-Sor Juana	+51, 27 W	–	–	–	–	–	560	(*810*)	–	–
Sobkou	+34, 132 W	–	–	–	(490)	–	850	[*1385*]	–	–
Brahms-Zola	+59, 172 W	–	–	–	325	–	620	(840)	[1080]	–
Donne-Molière	+04, 10 W	–	–	375	–	(*785*)	1060	(1500)	–	–
Hiroshige-Mahler	−16, 23 W	–	–	–	150	–	355	–	(700)	–
Mena-Theophanes	−01, 129 W	–	–	(260)	–	[475]	770	1200	–	–
Tir	+06, 168 W	–	–	380	660	950	1250	–	–	–
Budh	+17, 151 W	–	–	–	–	580	850	(1140)	–	–
Ibsen-Petrarch	−31, 30 W	–	–	–	–	425	640	(930)	[1175]	–
Andal-Coleridge	−43, 49 W	–	–	[420]	(700)	1030	1320	(1750)	–	–
Matisse-Repin	−24, 75 W	–	–	–	(410)	–	850	1250	[*1785*]	–
Bartok-Ives	−33, 115 W	–	–	(480)	–	790	1175	[1500]	–	–
Hawthorne-Riemenschneider	−56, 105 W	–	–	–	270	–	530	780	1050	–
Vincente-Yakolev	−52, 162 W	–	–	–	[360]	–	725	950	[*1550*]	–
Eitoku-Milton	−23, 171 W	–	(290)	–	590	(850)	1180	–	–	–
Sadi-Scopas	−83, 44 W	–	–	360	–	(600)	930	[1310]	–	–
Tolstoy	−16, 164 W	–	–	–	[260]	330	510	(720)	–	–
Caloris	+30, 195 W	–	–	–	[630]	(900)	1340	(2050)	[2700]	[3700]
Chong-Gauguin	+57, 106 W	–	220	350	–	[580]	(940)	–	–	–
Shakespeare	+49, 151 W	–	–	–	[200]	–	420	680	–	–
Van Eyck	+44, 159 W	–	–	–	150	–	285	[450]	[520]	–

Mars

Basin[b]	Center Coordinates (deg)	Mean observed ring diameters (km)[c, d]								
		"B"	"A"	I	II	III	IV	V	VI	VII
near Newcomb crater (1)	−22, 04 W	–	–	(290)	380	[580]	870	–	–	–
Ladon (3)	−18, 29 W	–	–	–	325	–	[*550*]	(760)	1000	(1600)
near Holden crater (4)	−25, 32 W	–	–	–	300	–	580	–	–	–
Chryse (5)	+24, 45 W	–	–	–	–	840	1320	1920	2840	[*3940*]
Mangala (6)	+00, 147 W	–	–	–	–	(500)	660	(1040)	–	–
Sirenum (7)	−44, 167 W	–	–	–	–	320	500	810	(1040)	–
so. of Hephaestus Fossae I (9)	−30, 180 W	–	–	[180]	–	290	440	–	–	(1540)
Al Qahira (10)	−20, 190 W	(125)	(210)	–	340	(490)	720	1140	–	–
so. of Hephaestus Fossae II (11)	−10, 233 W	–	–	(370)	(570)	–	1040	–	–	–
southeast of Hellas (12)	−58, 275 W	–	–	(200)	–	(360)	550	–	–	–
Nilosyrtis Mensae (13)	+32, 281 W	–	–	–	–	–	370	–	(720)	–
south of Renaudot crater (14)	+38, 297 W	–	150	–	(310)	(440)	660	–	–	–
south of Lyot crater (15)	+42, 322 W	–	–	145	200	260	400	(*565*)	–	–
Cassini (16)	+24, 331 W	–	–	150	200	(320)	430	–	950	–
Deuteronilus B (17)	+43, 338 W	–	44	–	–	130	200	–	(405)	–
Deuteronilus A (18)	+44, 342 W	44	–	80	–	140	220	[*290*]	–	–
near South crater (19)	−73, 214 W	–	–	–	(*385*)	–	(*740*)	1205	1315	[1890]
near Schiaparelli crater (20)	−05, 349 W	–	–	140	–	(300)	420	700	–	(1120)
near Le Verrier crater (21)	−37, 356 W	–	–	[190]	–	–	480	[640]	(850)	–
Noctis Labyrinthus (Schultz and Glicken, 1979)	−13, 105 W	–	–	–	(900)	–	(1800)	(2700)	(3900)	[5800]
South Polar (Croft, 1979)	−83, 267 W	–	–	–	(425)	(670)	850	–	–	–
Argyre	−50, 43 W	–	–	–	[410]	630	800	(1100)	(1360)	(1900)
Isidis	+13, 272 W	–	–	–	700	–	1500	–	3000	[3800]
Hellas	−41, 295 W	–	–	(840)	(1200)	(1700)	2200	3100	4400	[5500]
Huygens	−14, 304 W	–	–	–	240	340	465	–	–	–
near Cassini (Stam *et al.*, 1984)	+14, 324 W	–	–	–	(170)	(250)	355	[520]	[680]	(1100)

Table I (continued)

[a] Source: measured or remeasured by authors on spacecraft images, photomosaics, and maps, particularly after lists in Wilhelms (1984, Table 6.4), Schultz *et al.* (1982, Table 2), and Spudis (1984).
[b] Many names are provisional and do not constitute official nomenclature. Parenthesized identification numbers after Martian basins are those of Schultz *et al.* (1982, Table 2); their Arcadia (8) and Aram Chaos (2) basins exist, but the rings are too ambiguously defined for satisfactory measurements.
[c] Rings assigned to seven relative radial positions, or ranks, within each basin and two provisional ranks (see text). Weight values: [ ] = 1, ( ) = 2, all others = 3 (see text), reflect quality of observations.
[d] Italic printed diameters are weighted geometric means (in km) of two (in one case three) closely spaced (split) rings that occupy one rank (see text), as follows:

	Mean diameter	*Constituent Diameters*
Moon	*(1195)*	1120, (1340)
	[810]	[720], (850)
	[660]	(620), [740]
Mercury	*(810)*	(740), 890
	[1385]	[1280], 1420
	(785)	700, (825)
	[1785]	(1550), [1900]
	[1550]	(1250), (1700)
Mars	*[550]*	490, 570, 600
	(3940)	(3600), (4300)
	(565)	510, 620
	(290)	280, (312)
	(385)	360, 415
	(740)	685, 800

Wilhelms *et al.*, 1977) that rings outside the main rim may never have been as well expressed as those within. (We exclude rings perhaps accentuated by later endogenic development; Schultz, 1979.) Thus, rings of older, more degraded, basins may not always be visible, especially outside the main ring. The implication is that apparently 'missing' rings may well be present at older basins, but are not now recognizable.

2.2. TIR BASIN, MERCURY

Ancient, multi-ring basins on Mercury have been tabulated by Wood and Head (1976), Schaber *et al.* (1977), De Hon (1978), Frey and Lowry (1979), Croft (1979), Spudis (1984), and Spudis and Strobell (1984). They are recognized by four criteria: (1) isolated massifs and massif chains in circular patterns; (2) arcuate ridges aligned with massifs; (3) scarps aligned with (1) and (2) above; and (4) anomalously high terrain within the Mercurian inter-crater areas that align with all of the above. Most basins on Mercury are exceedingly degraded, and careful geologic mapping (Spudis and Prosser, 1984), assisted by topographic profiles from Earth-based radar (Spudis and Strobell, 1984), is required to establish their presence. The Mercurian measurements in Table I are largely from recent work by Spudis (1984).

The Tir basin lies within a structural trough associated with the Caloris basin, and is filled with smooth plains materials (Figure 2a, b). Tir is very old, predating the Mercurian intercrater plains, one of the oldest geologic units on the planet (Trask and Guest, 1975). Numerous massifs (Figure 2a, b) align with circular mare-type ridge patterns to outline the ancient structure of Tir. The mapping of basin-associated topographic and structural elements leads to the basin terrain map (Figure 2b). From these observations, rings are fitted that best explain the observed topographic pattern (Figure 2c).

Mapping the Tir basin illustrates several problems associated with determining precise ring diameters. Missing parts of rings (e.g. the northeast sector of the main ring), massif elements that lie outside an otherwise mapped ring (at $-02.5°$, 162.5° W.), and diverging ridge elements (at $+02°$, 174° W.) all contributed to errors in ring placement. Thus, our estimates of ring diameters (Table I) may be considered to carry a precision of $\pm$ ca. 50 km. for diameters on the order of 1000 km. We emphasize that these problems also attend rings even in the freshest basins (e.g. Cordillera ring of Orientale), so that the precision of ring data can be fairly similar from basin to basin.

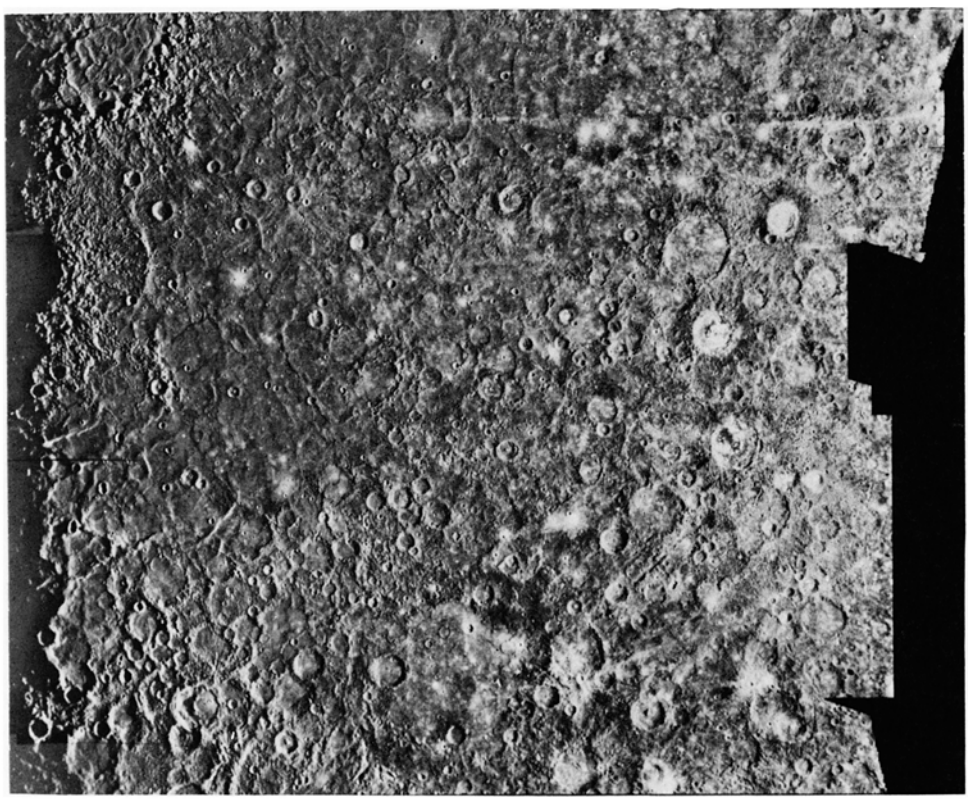

Fig. 2a. Site of the subdued Tir basin, Mercury. Rim of Caloris basin in upper left. Mariner 10 photomosaic of the Tolstoy (H-8) quadrangle of Mercury. Scene is 2000 km across; north at top.

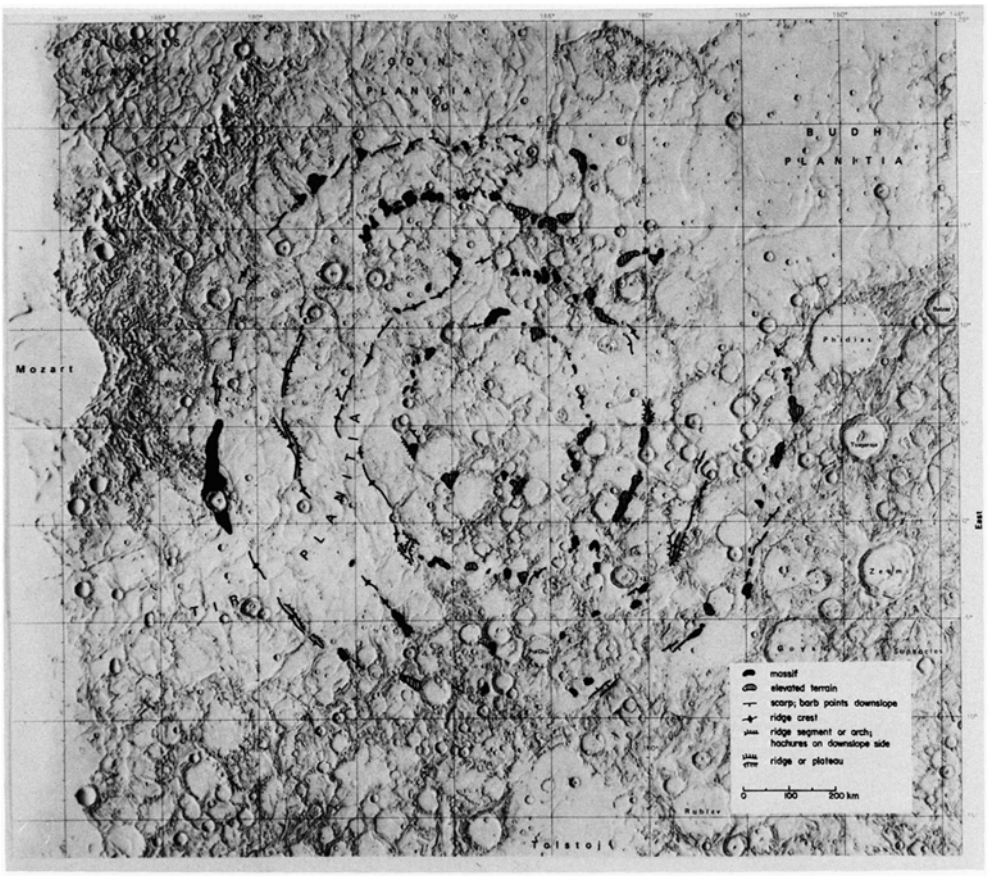

Fig. 2b. Terrain map of basin-associated elements for the Tir basin of Spudis (1984). Location of multiple rings indicated by massifs, mare-ridge alignments, and topographic highs. Base is part of shaded relied map of Tolstoy (H-8) quadrangle by U.S. Geological Survey.

2.3. AL QAHIRA BASIN, MARS

Schultz *et al.* (1982) first recognized the multi-ringed Al Qahira structure, along with 20 other large but fragmented basins on Mars (Figure 3). It lies within the southern uplands and has been degraded by large superposed impact craters and embayed by plains materials. Numerous large massifs and ridges within overlying smooth plains outline the structure (Figure 3a, b). Al-Qahira basin appears to have partly controlled the direction of subsequent large-scale channels, such as Ma'adim Vallis (Schultz *et al.*, 1982). Our ring interpretation (Figure 3c) is based on independent terrain mapping (Figure 3b), and thus the 112 Martian ring diameters in Table I differ somewhat from the 55 measured initially by Schultz *et al.* (1982). We also include two very small inner rings not listed by Schultz *et al.* (1982, Table II). Their omission would not affect the conclusions reached in this paper.

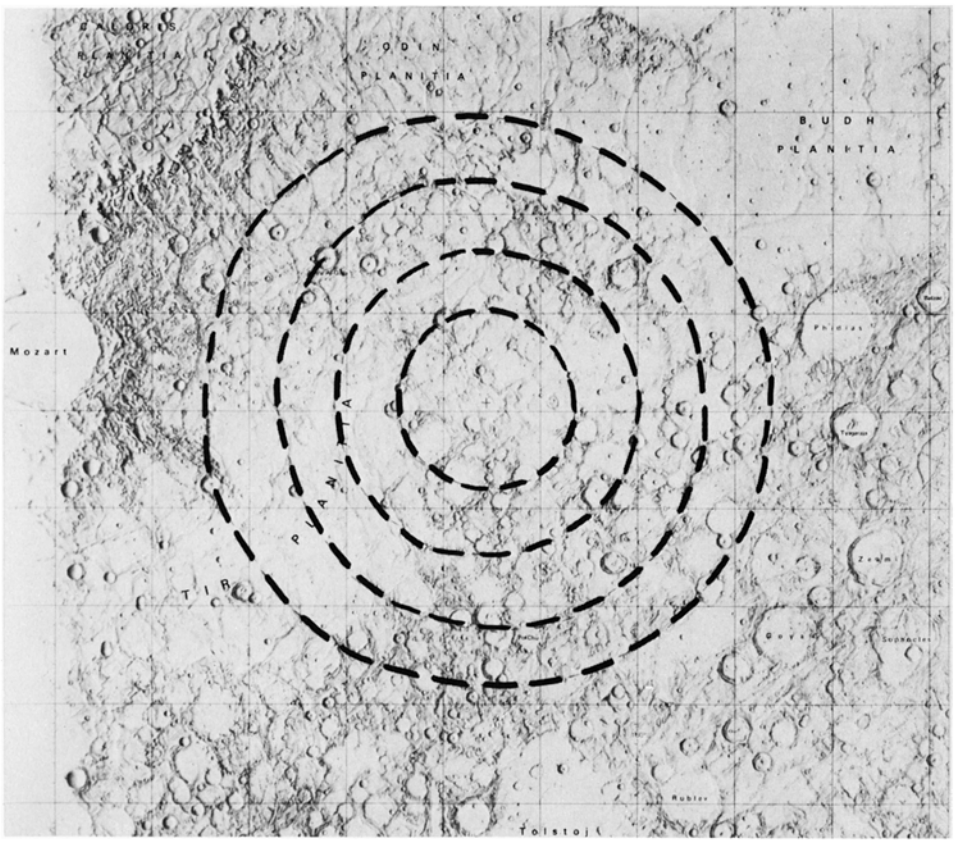

Fig. 2c. Four-ring interpretation of the Tir basin derived from terrain map in (b). Largest ring is 1250 km across (see Table I). Base map same as in (b).

Problems in mapping the Al Qahira basin resemble those encountered on both the Moon and Mercury. Because reliable topographic data are absent, the choice of the most prominent ring must rest on a qualitative, photogeologic assessment. In this case, the largest massifs appear to represent the original basin rim (720 km in diameter). Complicating the delineation of basin structure are groups of massifs, located between latitude $-26°$ and $-28°$ and W. longitude 185° to 187°, that may be related to another basin just to the south, centered at $-29.5°$, 180° W. (Schultz *et al.*, 1982). Unusually prominent massifs at $-21°$, 187° W. lie at the intersection of rings from both Al Qahira and the basin south of it. This topographic enhancement of intersecting rings and intervening troughs on Mars (Wilhelms, 1973), which is well known from lunar work (Wilhelms and McCauley, 1971), also may be observed at overlapping basins on Mercury. We found such enhancement to be an important tool in discovering additional basins.

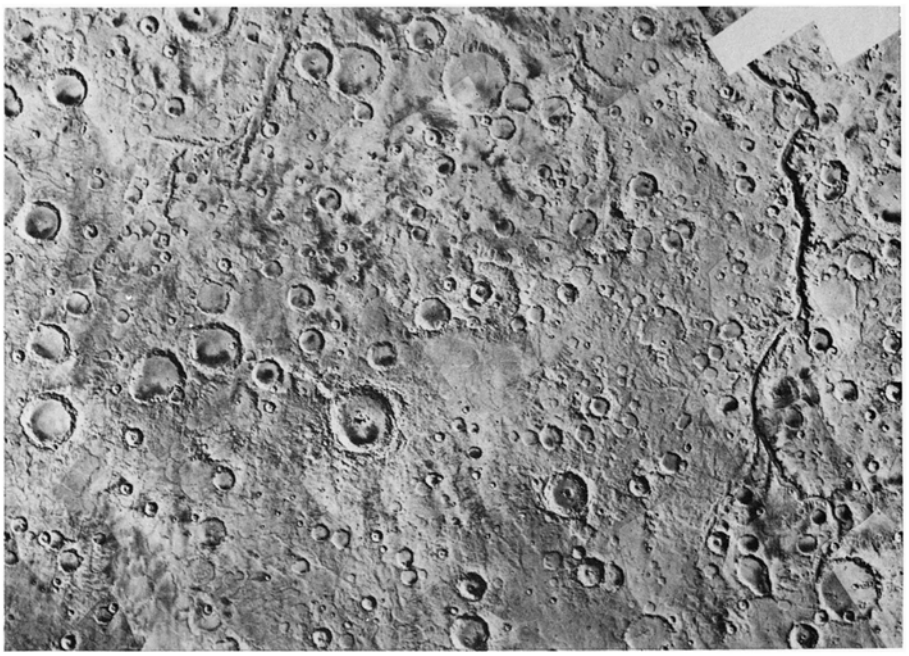

Fig. 3a. Site of southern two-thirds of the Al Qahira basin, Mars. Large channel at right is Ma'adim Vallis. Viking photomosaic of the MC-23 SE (Aeolis) quadrangle of Mars. Width of scene is about 1300 km; north at top.

2.4. Uncertainties in Measurement of Multiple Rings

The three multi-ring basins (Figures 1–3) illustrate various difficulties faced in assembling the sample of ring diameters from photogeologic evidence (Table I). For each of 67 basins we examined the available photographs and photomosaics, performed terrain mapping from the criteria described above, and attempted to fit circles that include most of the concentric features mapped. Because this sequence of steps will not lead to unique results in every case, some of our basin rings and/or their diameters differ from previously published results (cf. Schultz *et al.*, 1982; Croft, 1979; Wilhelms, 1984). Nonetheless, agreement between our estimates and those of others is substantial. For example, of the 55 Martian rings mapped by Schultz *et al.* (1982), 79% of our measured diameters lie within 10% of theirs. The different values for some basins partly reflect our access to more maps in the 1:2 000 000-scale Viking photomosaic series than were available for the earlier study by Schultz *et al.* (1982). Thus we consider our measurements in Table I to be as accurate as any others, considering the inherent uncertainties.

Three basins in Table I, Nilosyrtis Mensae and that near the crater Holden (Mars) and Derzhavin-Sor Juana (Mercury), have only two observed rings each. We include them because (1) the rings are so large that those basins almost certainly had at least

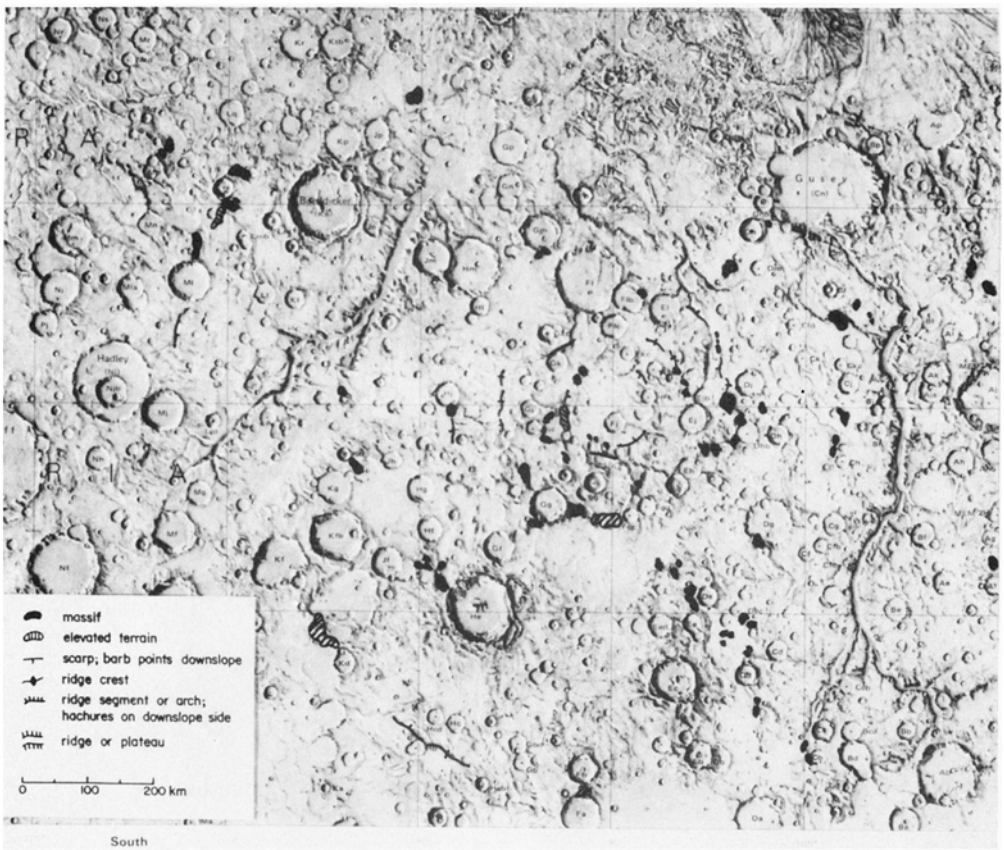

Fig. 3b. Terrain map of basin-derived features associated with the Al-Qahira basin of Schultz *et al.* (1982). Massifs and ridges outline the ancient basin rings. Base is part of shaded relief map (MC-23 quadrangle) by U.S. Geological Survey.

three rings initially (true two-ring basins are systematically smaller; see Table II), and (2) the second ring of two of these basins is larger than the main ring, not smaller as is observed for all true two-ring basins.

In some cases, two closely spaced rings or a group of ring arcs share one radial ring *position* in a basin. These 'split' rings have been described in basins on both the Moon (Wilhelms *et al.*, 1977; Wilhelms, 1980a) and Mars (Schultz *et al.*, 1982). One of the best examples of a split ring is in the Ladon Basin on Mars. Three closely spaced rings (Schultz *et al.*, 1982) make up the main rim of Ladon, as evidenced by topographic data from Earth-based radar (Saunders *et al.*, 1978). The chaotic arrangement of massifs that transect the split rings in many places suggests that the three rings are not separate and distinct. Similar geologic relations are evident within the Martian Argyre and lunar Crisium basins. We have computed the geometric mean for

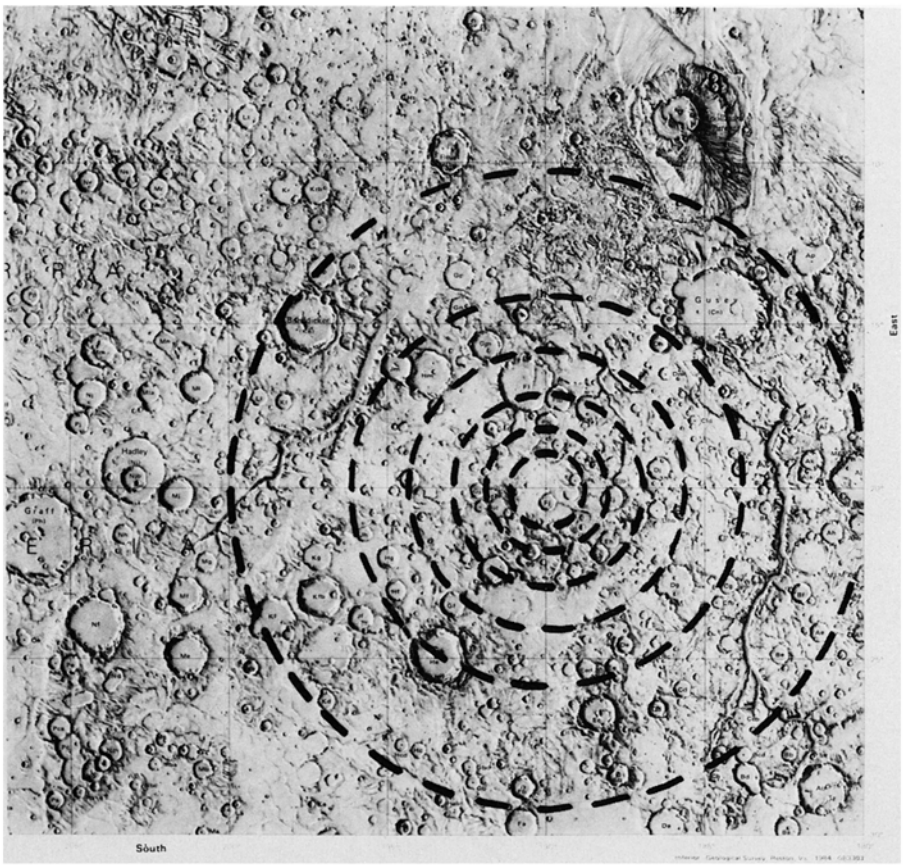

Fig. 3c. Six-ring interpretation of the Al-Qahira basin derived from terrain map in (b). Largest ring is 1140 km in diameter (see Table I). Base map same as in (b). Evidence for two smallest rings, not mapped by Schultz *et al.* (1982), appears in (b) from interpretation of physiography in (a).

diameters of broken arcs to assign a single diameter to split rings. This averaging introduces observational bias into the statistical analysis of ring spacing, but it is minimal *because split rings are such a small percentage (about 5% of the rings of just multi-ring basins) of the total sample.*

2.5. Two-ring basins and protobasins

Concentric structures with fewer than three rings pose greatly reduced problems of recognition and measurement compared to those attending multi-ring basins. Consequently, most two-ring structures in Table II are well known from past work, and their diameters are uncontroversial. We examined on images and maps all two-ring basins (Figure 4) and protobasins (Figure 5) listed previously for the Moon, Mercury, and Mars (e.g., Croft, 1979; Wood, 1980; Wilhelms, 1984), checking and

TABLE II

Ring diameters of 97 protobasins and two-ring basins[a]

Protobasins						Two-ring basins				
Name	Center coordinates (deg)	Observed diameter[b]				Name	Center coordinates (deg)	Diameter[b]		
		Rim	Inner ring	Base of central peak	W[c]			Rim	Inner ring	W[c]
					Moon					
Antoniadi	−70, 188 E	135	60	8	(3)	Amundsen-				
Bailly	−07, 291 E	290	125	–[d]	(3)	-Ganswindt	−81, 120 E	355	175	(1)
Campbell	+45, 153 E	230	90	9	(2)	Birkhoff	+59, 214 E	325	150	(1)
Compton	+56, 105 E	175	75	20	(3)	Lorentz	+34, 263 E	365	170	(3)
D'Alembert	+51, 165 E	237	95	–	(3)	Planck	−58, 136 E	325	160	(1)
Fermi	−20, 123 E	238	90	40	(2)	Poincaré	−57, 164 E	325	160	(1)
Gagarin	−20, 149 E	272	110	–	(2)	Schiller-				
Hipparchus	−06, 05 E	151	58	9	(1)	Zucchius	−56, 316 E	335	175	(3)
Janssen	−45, 42 E	180	70	–	(1)	Schrödinger	−76, 134 E	320	150	(3)
Landau	+43, 241 E	221	90	–	(1)					
Mendeleev	+06, 141 E	365	140	21	(2)					
Milne	−31, 113 E	262	108	–	(2)					
Oppenheimer	−35, 194 E	215	85	–	(1)					
Pasteur	−11, 105 E	245	85	–	(1)					
Schickard	−44, 306 E	227	87	–	(2)					
Schwarzschild	+71, 120 E	220	80	–	(3)					
Zeeman	+75, 225 E	184	74	–	(1)					

Table II (continued)

Mercury

–	−28, 20 W	72	36	7	(2)	Ahmad Baba	+59, 127 W	132	60	(3)
–	+01, 17 W	76	25	15	(3)	Al-Hamadhani	+39, 90 W	155	75	(3)
–	+13, 27 W	95	32	15	(2)	Bach	−69, 103 W	210	103	(3)
Asvaghosa	+11, 21 W	86	29	13	(3)	Botticelli	+64, 110 W	148	70	(2)
Bernini	−79, 135 W	165	65	10	(3)	Cervantes	−75, 122 W	203	106	(3)
Boethius	−01, 74 W	122	50	12	(3)	Chekhov	−36, 62 W	205	100	(3)
Brunelleschi[e]	−09, 23 W	128	34	17	(3)	Dorsum Schiaparelli Basin	+17, 166 W	225	120	(2)
Chong Chol	+47, 116 W	138	58	11	(2)	Dürer	+22, 119 W	190	95	(3)
Equiano	−39, 31 W	105	46	18	(2)	Handel	+04, 34 W	153	68	(2)
Hawthorne	−51, 116 W	125	55	25	(2)	Hitomaro Basin	−15, 15 W	255	125	(3)
Hitomaro	−16, 16 W	115	40	14	(3)	Homer	−01, 37 W	310	172	(2)
Jo' Kai	+73, 136 W	86	38	12	(3)	Ma Chih-Yuan	−59, 78 W	190	90	(3)
Lu Hsun	00, 24 W	101	41	22	(2)	Mark Twain	−11, 138 W	150	80	(2)
Mansur	+48, 163 W	95	38	12	(2)	Mendes-Pinto	−61, 20 W	195	100	(2)
Scarlatti	+40, 100 W	152	69	6	(3)	Michelangelo	−45, 110 W	225	105	(3)
Sinan	+16, 30 W	136	60	7	(3)	Mozart	+08, 191 W	255	130	(3)
Ts'ai Wen Chi	+23, 23 W	123	54	14	(3)	No. Pole Basin	+85, 171 W	170	85	(2)
Van Gogh	−76, 136 W	98	37	18	(2)	Pushkin	−65, 24 W	235	125	(3)
Verdi	+65, 169 W	140	50	35	(1)	Renoir	−18, 52 W	225	110	(3)
Zeami	−03, 147 W	130	44	12	(1)	Rodin	+22, 18 W	235	117	(3)
						Shelley-Delacroix Basin	−48, 136 W	222	105	(2)
						Sotatsu	−48, 19 W	160	74	(2)
						So. of Molière	+10, 16 W	295	145	(1)
						Strindberg	+54, 134 W	190	90	(2)
						Surikov	−37, 125 W	235	110	(2)
						Valmiki	−23, 142 W	210	105	(2)
						Vivaldi	+14, 86 W	205	100	(3)
						Vyasa	+49, 81 W	280	145	(1)
						Wang Meng	+09, 104 W	165	80	(3)
						Wren	+25, 36 W	208	120	(2)
							+48, 169 W	175	80	(2)

Table II (continued)

Mars										
22-Gt	−09, 237 W	64	26	11	(3)	5-Kd	+35, 325 W	96	46	(3)
Bakhuysen	−22, 344 W	153	60	32	(2)	12-Xq	+16, 355 W	52	24	(2)
Barnard	−61, 298 W	123	39	24	(3)	16-Re	−25, 164 W	151	68	(3)
Bjerknes	−43, 189 W	90	35	17	(2)	16-Qg	−23, 163 W	57	27	(1)
Holden	−26, 34 W	147	61	20	(1)	20-Yp	−13, 357 W	70	38	(3)
Liu-Hsin	−55, 172 W	135	51	23	(3)	22-Dt	−09, 231 W	90	41	(2)
Trouvelot	+16, 13 W	148	58	18	(1)	Arrhenius	−40, 237 W	122	70	(2)
						Galle	−51, 31 W	214	104	(2)
						Kaiser	−46, 341 W	204	100	(1)
Herschel[f]	−15, 230 W	301	145	40	(2)	Kepler	−47, 219 W	224	122	(3)
Lyot[f]	+51, 331 W	224	113	27	(2)	Lowell	−52, 81 W	198	94	(3)
						Molesworth	−28, 211 W	179	91	(3)
						Phillips	−67, 45 W	175	90	(2)
						Ptolemaeus	−47, 158 W	167	78	(3)
						Schiaparelli	−03, 343 W	442	225	(3)

[a] Source: measured or remeasured by authors on spacecraft images, photomosaics, and maps, mostly after lists of Wood and Head (1976, Table 2), Croft (1979, Tables 5.1–5.3), Wood (1980, Table 1), and Pike (1983, Figure 1).

[b] Values for rim and inner ring are means; values for peak base are maxima (Hale and Grieve, 1982).

[c] Weight values (see text; cf. Table I) reflect quality of observations.

[d] Central peaks not observed (probably buried) for 11 presumed protobasins, which were recognized on basis of high D/D_i, morphologic dominance of rim over inner ring, and D range: ≥ Antoniadi but ≤ Mendeleev.

[e] Unusally small inner ring possibly an open or expanded cluster of central-peak elements (Pike, 1983).

[f] 3rd ring between D and D_i, 220 km (Herschel) and 158 km (Lyot), thus making these anomalous features 'multi-ring protobasins'; omitted from statistics.

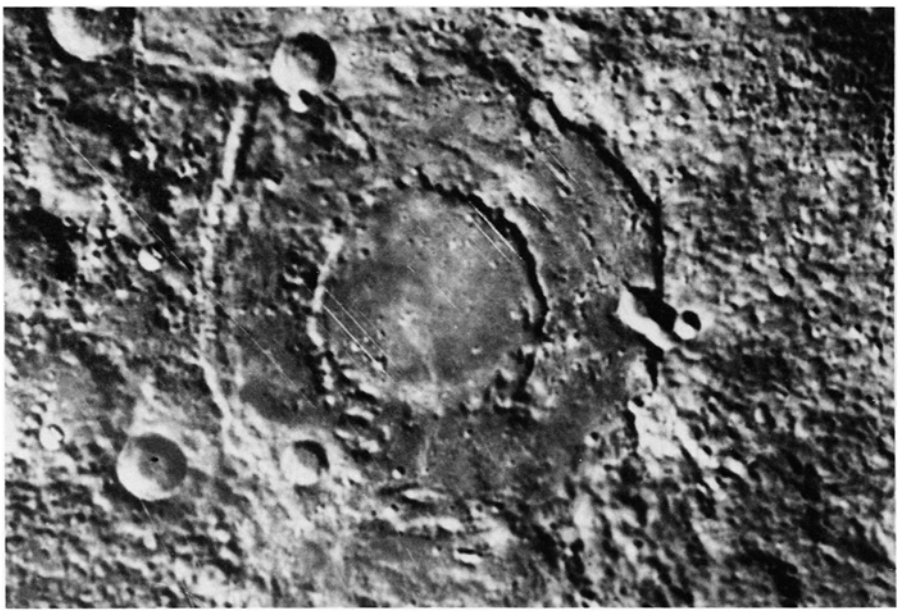

Fig. 4. The two-ring basin (alternatively 'peak-ring basin') Bach, 210 km across at − 69°, 103° W, on Mariner-10 photomosaic 15-C (Davies *et al.*, 1976), of the Bach area of Mercury (see also Spudis and Prosser, 1984). Similar two-ring basins are observed elsewhere on Mercury and on the Moon and Mars (Table II). North at top.

remeasuring the diameters of both rim and inner ring (Table II). Ring diameters were easier to define accurately and precisely (generally less than about ± 5% D) than were those of multi-ring basins, because most two-ring structures are so much smaller, more continuous, and (usually) younger and less degraded. Inner rings of protobasins such as Van Gogh on Mercury (Figure 5), may be incomplete and thus difficult to measure accurately. Their central peaks are unusually small (Pike, 1982, 1983), and can be absent entirely (Table II; Pike, 1983). The inner ring of the two-ring basin Bach, on Mercury (Figure 4), is complete and exceptionally conspicuous, which is not always the case (cf. the Moon; Wilhelms, 1984). As more and better source materials have become available, especially for Mars, we discarded some structures as lacking definable and measurable inner rings (e.g., Mie, Moreaux, and Gale) and added others for which good data could be obtained unambiguously (e.g., Bjerknes, Trouvelot, and 22-Dt). Similarly, at least three rings now are mapped for the formerly two-ring lunar basins Korolev, Apollo, and Balmer (Table I).

3. Ring Observations and Their Weighting

The raw data are average diameters of 490 rings mapped by the foregoing procedures for 164 basins and protobasins on the Moon, Mars, and Mercury. Protobasins

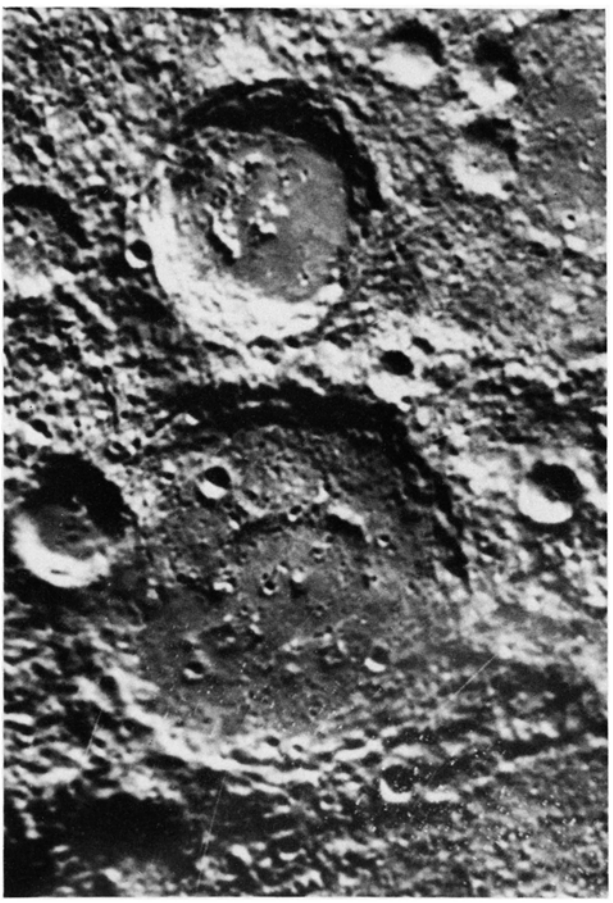

Fig. 5. Two protobasins (alternatively 'central-peak basins'), large impact craters that have a small central peak and a small inner ring. Van Gogh, 98 km across at − 76°, 136° W, and Bernini, 165 km across at − 79°, 135° W, both on Mariner-10 photomosaic 15-B (Davies *et al.*, 1976), of the Bach area of Mercury. Similar protobasins are observed elsewhere on Mercury (e.g., De Hon *et al.*, 1981) and on the Moon and Mars (Table II). North at top.

(n = 44) and two-ring basins (n = 53) account for 194 rings (Table II). The 67 multi-ring basins share the remaining 296 rings (Table I). Ring ranks, radial positions of rings within each multi-ring basin, are explained below. Each ring diameter (inner and outer rings together for two-ring basins) also is assigned a relative weight of 1, 2, or 3 for subsequent analysis. The weighting value reflects both (1) likelihood that the ring exists, and (2) accuracy with which the ring could be measured, and thus it roughly indicates the ring's physiographic prominence. Some low weights simply reflect poor photographs and images. The diameters of most of the doubtful, or 'weakest', rings in Table I (weight = 1) are bracketed, and those of only 'moderately strong' rings (weight 2) are parenthesized; the remainder are diameters of the

'strongest' rings, in which we have the most confidence (weight 3). Weights are listed separately in Table II. The relative weights are roughly comparable from planet to planet.

Fourteen ring positions in Table I contain two and in one case (Mars) three split segments, whose individual diameters are given in a footnote. The presence of split rings reduces 296 *mapped* rings to 281 *ranked* rings (We recognized split rings *before* the ranking step). Geometric mean diameters of split rings were calculated from the constituent diameters using the 1-2-3 weights. In subsequent calculations, split basin rings are assigned the weight of the weaker constituent. The weighting is purposely conservative to reflect the uncertainties inherent in measuring split rings and partial arcs.

4. Multiple-Ring Position and Ring Rank

The rings of two-ring basins and protobasins clearly are either 'outer' (main) or 'inner'. This lack of ambiguity does not extend to multi-ring basins. Therefore, rings of each multi-ring basin are assigned a numerical rank that corresponds to their relative radial position (Pike, 1981; Pike and Spudis, 1984a, b). Ranking enables the rings of many basins, including those with only two rings, to be combined in testing for statistical and spatial regularities (Wilhelms *et al.*, 1977; Croft, 1981b; Schultz *et al.*, 1982). Its effects are twofold: (1) Ranking facilitates comparisons among basins, by establishing a simple geometric correspondence of rings referenced to the most important ring in each basin. (2) Ranking surmounts the problem of possibly 'missing' rings, which severely complicates any type of statistical analysis of ring spacing (see discussion in Sections 5.1.2. and 5.1.3.), by establishing for each basin a similar suite of *ring positions*, which may or may not be 'filled' by observed features.

4.1. Rationale and Procedure

The basis for ranking the rings of multi-ring basins (Pike, 1981) derives from four observations, first made on lunar data: (1) adjacent rings of the fresh Orientale basin and the older basins Nectaris, Humorum, and Imbrium are spaced almost exactly at $2.0^{0.5}$D (Fielder, 1963; Van Dorn, 1968); (2) many rings of other, less well preserved, basins on the Moon have approximately this same spacing (Hartmann and Kuiper, 1962); (3) non-$2^{0.5}$D spacing intervals, commonly 2.0D, tend to be integer multiples of $2^{0.5}$D (Hartmann and Kuiper, 1962; Hartmann and Wood, 1971), rather than some unrelated value; and (4) one ring in a basin tends to be more prominent than the others (Hartmann and Wood, 1971).

The 281 ranked rings of the 67 multi-ring basins belong to at least seven well-defined groups of ring diameters (Figures 6–8, Table I). Spacing *between adjacent ring groups* increases incrementally outward by about $2^{0.5}$D or an integer multiple of it. This value was first proposed for ring spacing of the four lunar basins measured in Hartmann and Kuiper (1962) by Fielder (1963), in a seldom-cited paper in which

he interpreted basin rings as endogenic. Hartmann and Kuiper (1962) themselves had given the interval virtually the same value, '... about 1.5 D ...'

We recognized groups of ring diameters and their constant spacing on separate planets from graphic analysis of *combined* data for many multi-ring basins (Figures 6–8). Each ring (diameter = D_n) in a basin was assigned a rank number on a common assumption and observation: One ring (diameter = D_m), rather more prominent and/or continuous than the others (see Hartmann and Wood, 1971, Table II and Figure 27 and discussion in Hodges and Wilhelms, 1978, and Schultz *et al.*, 1982), is equivalent to the rim crest of nonringed craters, up to the size of protobasins on that planet. The topographically 'strongest' ring is the 'main ring' or 'topographic rim' (e.g. Cordillera of Orientale). Its selection, made only after all rings of that basin had been mapped and measured, usually was straightforward but can be equivocal in the case of degraded basins.

Plotting ring diameter, D_n, against that of the main ring, D_m, for each multi-ring basin, in the log D domain (after Figure 11 of Wilhelms *et al.*, 1977) separates most of the observed rings into linear concentrations of points (Figures 6a–8a). (Comparison of the diameter of any basin ring with that of the main ring originated with Hartmann and Wood, 1971, Figure 27; the log D transformation is required by skewness of both variates toward high values; Baldwin, 1949.) The resulting point clusters are subparallel, slope at about unity, and are spaced at similar intervals, about $2^{0.5}$D. That the $2^{0.5}$D interval is optimum for these data is immediately evident by overlaying Figures 6a–8a with different templates of equispaced parallel lines. More points lie close to lines with the $2^{0.5}$ spacing than they do for any other. The linear groups of basin rings are most discrete on the Moon and least discrete on Mars. Our assignments of outliers, ambiguous points between two distinct clusters, to one group or the other were aided by (1) drawing a polygon around each cluster and/or (2) fitting it visually with a least-squares line. The number of points in each cluster ranges from one to 18.

4.2. Resulting Ranks of Multiple Rings

The D_n/D_m plots in Figures 6a–8a reveal six principal groups of rings for multi-ring basins on each planet. Probably one (all three bodies) and perhaps two (Mars only) more small ($n = 2$ or 3) groups lie at the lower end of the diameter range (columns 'A' and 'B' in Table I). A seventh principal cluster, which falls in the middle of the other six and thus occupies the fourth position, is simply the strongest ring plotted against itself. The resulting three sets of plots constitute empirical statistical models for average basin-ring spacing on the Moon, Mercury, and Mars. The three patterns are similar, including the observation that the uppermost ring group is the weakest.

The seven D_n/D_m distributions of basin rings in Figures 6a–8a are numbered I–VII, in order of increasing ring size on the vertical axis, in Figures 6b–8b. The main ring, or topographic rim (D_m), thus is IV. The corresponding taxonomy followed here for the six other ring groups is: (I) inner, (II) 'peak' (sic), (III) intermediate, (V) outer-1, (VI) outer-2, and (VII) outer-3. The equivalent ring

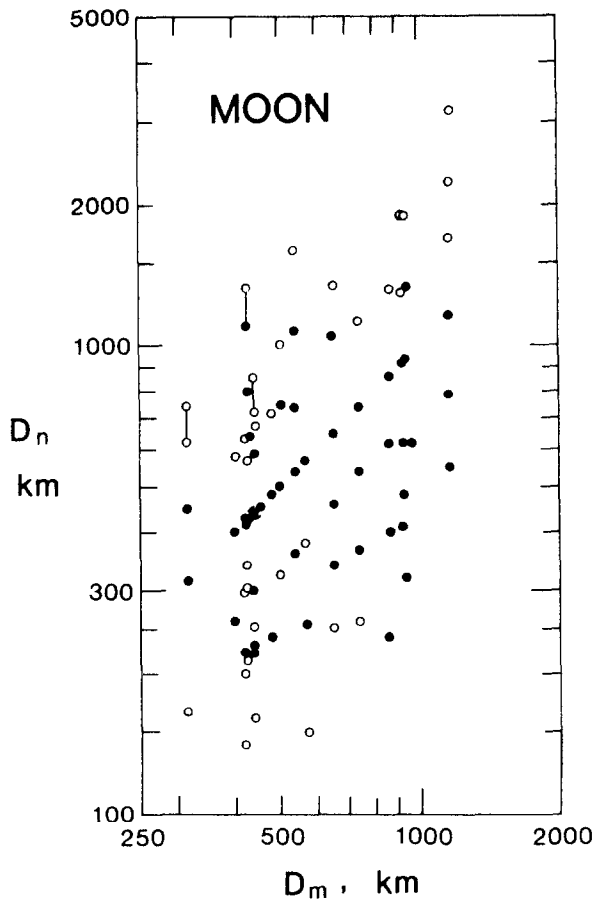

Fig. 6a. Ring-diameter correlations for 18 lunar multi-ring basins: unranked observations. Dots: diameter of each ring in a basin, D_n, plotted against that of the main ring, D_m (Table I). Circles: diameters of partial arcs and less-certain rings. Short vertical lines join two closely spaced rings or arcs, presumably split segments of one ring (see text). Discreteness of linear clusters most evident here, least so for Mars. Compare with Figures 7a and 8a.

diameters are $D_{\text{I...VII}}$. This system is provisional in that the possible ring cluster below rank I on all three planets ('A') may eventually warrant the I designation, in which case the main ring would become ring V.

Seven $D_{\text{I-VII}}/D_{\text{IV}}$ ring positions are not evident on all planetary bodies. Only abbreviated versions of the same patterns have been identified elsewhere, presumably because the available measurements are far fewer. The five multi-ring basins thus far discovered on the outer-planet satellites Rhea, Tethys, and Ganymede have a total of only 24 rings, which appear to occupy six clusters (Moore *et al.*, 1984). The 26 structural and topographic rings of the six terrestrial impact structures that contain three or more rings belong to just five groups (Pike, 1985).

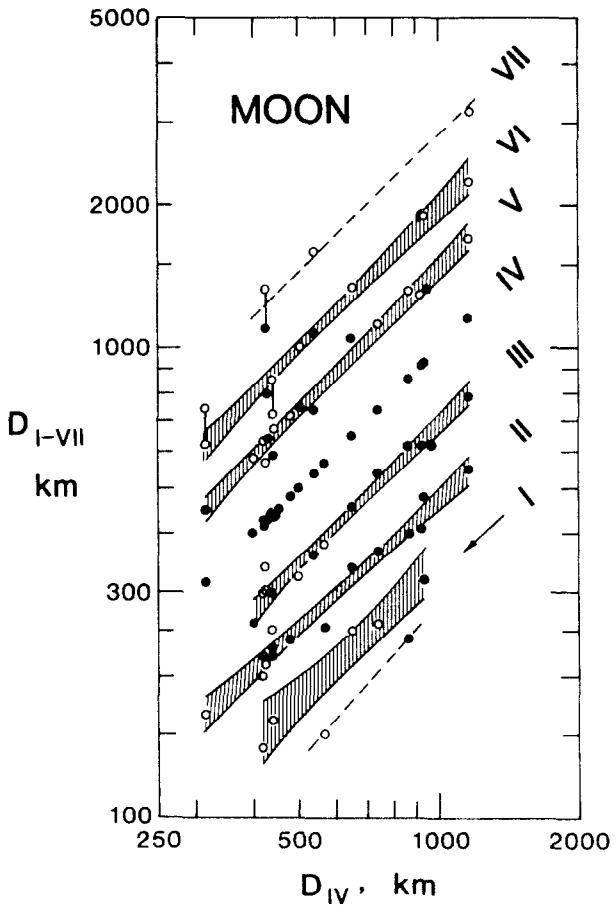

Fig. 6b. Resultant ring ranks for the Moon. Dots: basin ring diameter, $D_{I...VII}$ ($n = 85$), as a function of main-ring diameter, D_{IV} (Table I), plotted in (a). Shaded pairs of curves enclose 95% confidence intervals for linear fits to five of the six major clusters of rings (C.I. not plotted for rank VII, where $n < 5$; upper dashed line is equation). Analysis of covariance shows that adjacent equations here and in Figures 7b and 8b differ significantly at 1%. Least-squares fits, (Table III) slope at about unity and are spaced at about $2^{0.5}$D intervals. Intervals III–IV and IV–V are slightly wider here, also on Mercury (Figure 7b) and Mars (Figure 8b). Two points belong to a rank below I (lower dashed line). Partial arcs and less-certain rings (circles) weighted less in correlations. Split segments (joined by short vertical lines, as in a), which occupy the same rank in a basin (see text), have been averaged for least-squares fits. Compare with Figures 7b and 8b.

At least five of the ring groups derived in Figures 6–8 may be familiar from previous work, especially on the Moon, although true and detailed 'structural equivalence' (e.g., Croft, 1979, p. 135; Schultz *et al.*, 1982, Figure 10) is less easily established (see discussion in Pike, 1985). Our ranks II–VI are essentially the five clusters of lunar rings evident in Figure 27 of Hartmann and Wood (1971) and in Figure 6 of Howard *et al.* (1974). The same five ranks also seem to be the classes of

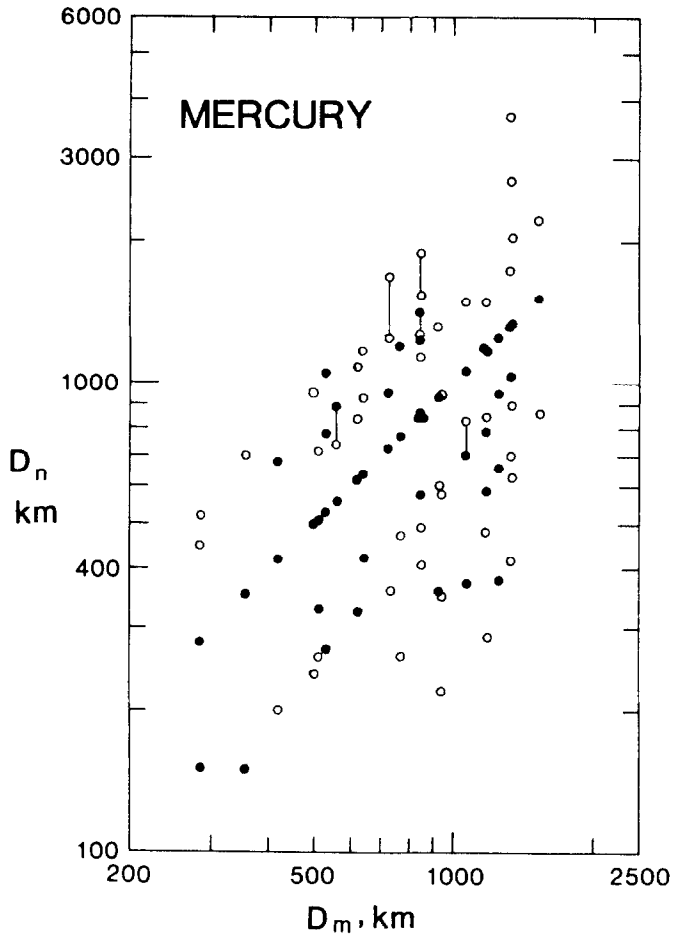

Fig. 7a. Ring-diameter correlations for 23 multi-ring basins on Mercury: unranked observations. Dots: diameter of each ring, D_n, as a function of main-ring diameter, D_m (Table I). Circles are partial arcs and less certain rings. Short vertical lines are split rings. Linear clusters less distinct here than on the Moon, but more so than on Mars. Compare with Figures 6a and 8a.

lunar rings identified by Wilhelms *et al.* (1977, Figure 11), whose broad 'inner ring' group is equivalent to both ranks II and III in our scheme. Ring ranks II, III, and IV correspond, respectively, to the lunar 'central-peak' ring, intermediate ring, and 'outer' ring of Head (1977a). Our ranks I–V also correspond to the six lunar classes of Croft (1981a), his two types of 'intermediate' rings being equivalent to our rank III. The sixth, and especially the seventh, ranks commonly are tenuous and fragmentary outer arcs whose lunar counterparts may be represented by the 'outer ring' of Imbrium (Wilhelms and McCauley, 1971) and our ring VI of Orientale. These two ranks also are less common than most (Croft, 1981a), especially VII on Mercury and the Moon.

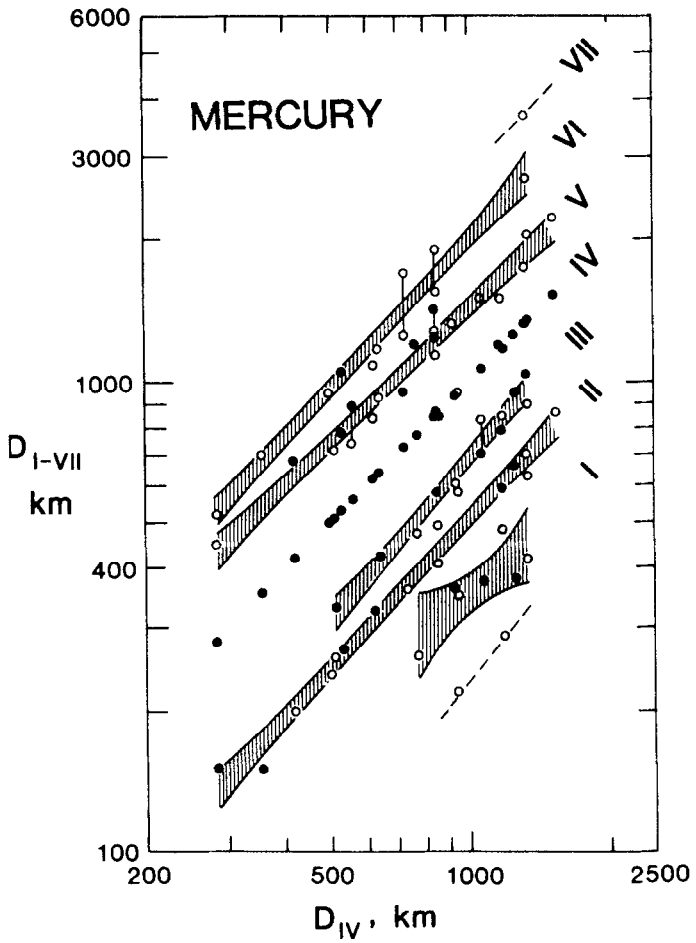

Fig. 7b. Resulting ring ranks for Mercury. Dots: basin ring diameter, $D_{I...VII}$ (n = 92), as a function of main-ring diameter, D_{IV} (Table I), plotted in (a). Shaded pairs of curves enclose 95% confidence intervals for linear fits to the five major clusters of rings. Least-squares fits, spaced at roughly $2^{0.5}$D intervals, are given in Table III. The greater width of intervals III–IV and IV–V is most evident on Mercury. Ring VII is represented by one point only (upper dashed line: not a mathematical fit); two low points belong to a rank < I (lower dashed line). Partial arcs weighted less in fits (see text). Split rings and arcs (see text) averaged for least-squares fits. Compare with Figures 6b and 8b.

Three general relations are evident among the 281 ranked rings for the multi-ring basins in Table I: (1) those outside the main ring (n = 93) are only 1/4 less frequent than those within (n = 121); (2) 70% to 100% of the rings in ranks V to VII are weighted '1' or '2', whereas only 45% to 60% of those in ranks I to III carry such low weights; and (3) split exterior rings are much more common (11%) than split interior rings (2%). The first observation is particularly important: It suggests that exterior rings are nearly as prevalent as interior ones, despite their weaker

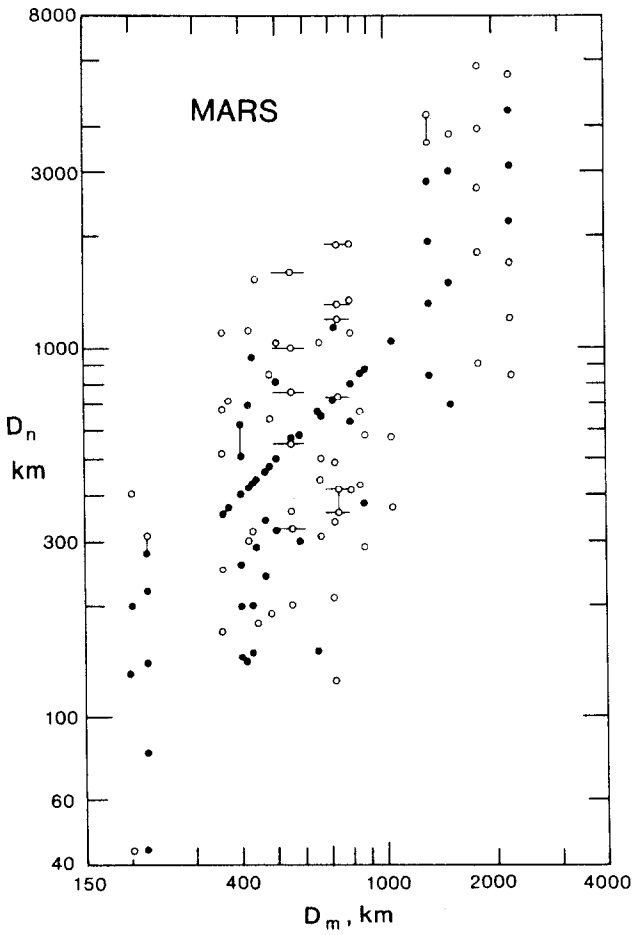

Fig. 8a. Ring-diameter correlations for 26 multi-ring basins on Mars: unranked observations. Dots: ring diameter, D_n, plotted against main-ring diameter, D_m (Table I). Circles are partial arcs and less certain rings. Short vertical lines are split rings; short horizontal lines bracket mean D_{IV} values derived from two or three closely spaced rings. Linear clusters less discrete here than on the Moon and Mercury. Compare with Figures 6a and 7a.

topographic expression, and thus that *any explanation for ring spacing must be equally plausible for rings in both locations.* The second relation introduces some measure to the well-known qualitative observation that physiographic prominence of rings decreases with increasing rank. Finally, our data indicate that prevalence of split rings increases with rank, even within interior and exterior groups: from 0% at ranks < I and I to 2% at II and III, and from 8% at rank V to 13% and 14% at VI and VII (3% of rank IV rings are split). Thus exterior rings are much more prone to splitting than interior rings, as well as being more vaguely defined. We examine the implications of this relation for process at the close of the paper.

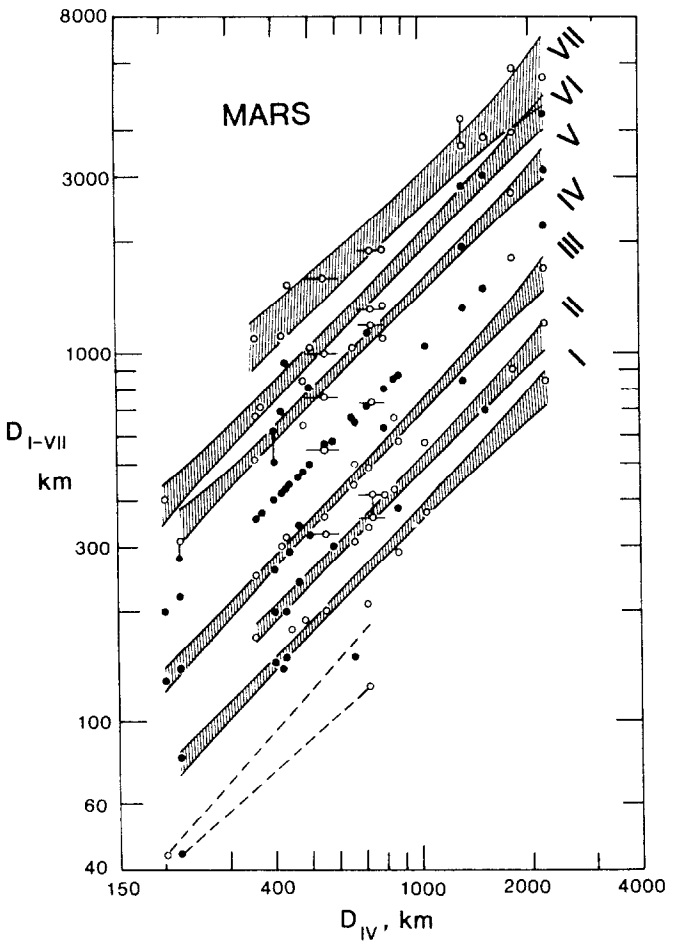

Fig. 8b. Resulting ring ranks for Mars. Dots: basin ring diameter, $D_{I...VII}$ ($n = 119$), as a function of main-ring diameter, D_{IV} (Table I), plotted in (a). Shaded pairs of curves enclose 95% confidence intervals for linear fits to the six major clusters of rings (five low 'orphan' points belong to two ranks $< I$ – dashed lines). Least-squares fits, spaced at roughly $2^{0.5}$ intervals, are given in Table III (intervals for ranks III–IV and IV–V are wider). Partial arcs weighted less, and split rings were averaged for fits. Compare with Figures 6b and 7b. Regressions differ significantly at the 1% level.

5. Statistics of Ring Spacing

This section presents a thorough treatment of ring spacing by simple statistics of central tendency and dispersion, using three different approaches. The parallel analyses are not redundant, but rather extract the maximum amount of information from the large sample of basins and protobasins. We computed mean spacing and its standard deviation and/or 95% confidence interval for ranked rings arranged in three ways: (1) by groups of similarly ranked diameters correlated with those of basin

main rings, (2) as diameters correlated with rank number for each basin (multi-ring basins only), and (3) as ratios of diameters of adjacent and alternately ranked rings. The resulting values of ring spacing were converted to a common variable, x, which enables spacings to be compared directly, regardless of their actual values. Results of the three complementary approaches for both multi-ring and two-ring structures yield a mean increment of ring spacing, $\bar{x}$, of $(2.0 \pm 0.3)^{0.5}$D, at 95% C.I. on each planet. Protobasins, however, differ significantly; their $\bar{x} = (3.3 \pm 0.6)^{0.5}$D at 95% C.I.

5.1. Least-squares groups of ranked rings

The first analysis of ring spacing follows immediately from the method by which ring ranks were recognized for multi-ring basins (Figures 6–8). It determines the spacing between each ring group and the main basin ring (Table III), and then repeats the calculations for paired *adjacent* groups of multiple rings (Table IV). A similar treatment of least-squares groups of ring diameters for two-ring basins and protobasins (Figure 10, Table V) is deferred to Sections 5.1.3 and 5.1.4.

5.1.1. *Adjacent Ring Positions of Multi-Ring Basins*

We summarized each D_n/D_m distribution in Figures 6a–8a statistically and evaluated the dispersion of the data by linear least-squares analysis (minimum $n = 3$), in the log D domain, at the 95% confidence interval in Table III. The C.I. envelopes

TABLE III

Spacing of basin rings referenced to main ring, from linear least-squares fits to diameters of rings grouped by rank: multi-ring basins

Results of regression analysis[a]					Statistics of ring spacing				
Ring groups[b]	a	r[b]	b, Slope	a, Y_c at $X=1$ km, km	Y_c, 95% C.I. at $\bar{X}_g$, km[c]	$Y_c/\bar{X}_g$, 95% C.I. Model	$Y_c/\bar{X}_g$, 95% C.I. Observed	Form[d]	Observed x, 95% C.I.[e]
					Moon				
'A'/IV[f]	2	–	–	–	–	0.250	0.27 –	$x/8$	2.4
I/IV	5	0.99	0.969 ± 0.273	0.434	223^{+19}_{-18}	0.354	$0.357^{+0.031}_{-0.029}$	$x^{0.5}/4$	$2.035^{+0.369}_{-0.318}$
II/IV	15	0.99	0.912 ± 0.093	0.873	300 ± 10	0.500	$0.496^{+0.017}_{-0.016}$	$x/4$	$1.971^{+0.138}_{-0.127}$
III/IV	14	0.99	1.006 ± 0.082	0.662	469^{+14}_{-13}	0.707	0.688 ± 0.020	$x^{0.5}/2$	$1.895^{+0.113}_{-0.107}$
IV/IV	18	–	(1.000)	(1.000)	592	1.000	(1.000)	$x/2$	(2.000)
V/IV	16	0.99	1.014 ± 0.082	1.336	881 ± 27	1.414	$1.457^{+0.045}_{-0.044}$	$x^{0.5}$	$2.124^{+0.134}_{-0.126}$
VI/IV	9	0.99	1.026 ± 0.087	1.679	1200^{+41}_{-40}	2.000	$1.984^{+0.068}_{-0.066}$	x	$1.969^{+0.138}_{-0.129}$
VII/IV	3	0.99	0.97 ± 0.95	3.4	1997^{+989}_{-662}	2.828	$2.8^{+1.4}_{-0.9}$	$2x^{0.5}$	$2.0^{+2.5}_{-1.1}$

Table III (continued)

Results of regression analysis[a]					Statistics of ring spacing				
Ring groups[b]	a	r^b	b, Slope	a, Y_c at $X=1$ km, km	Y_c, 95% C.I. at $\bar{X}_g$, km[c]	$Y_c/\bar{X}_g$, 95% C.I. Model	$Y_c/\bar{X}_g$, 95% C.I. Observed	Form[d]	Observed x, 95% C.I.[e]
Mercury									
'A'/IV[f]	2	–	–	–	–	0.250	0.24 –	$x/8$	1.8 –
I/IV	7	0.81	0.798 ± 0.601	1.437	359^{+72}_{-34}	0.354	$0.356^{+0.037}_{-0.034}$	$x^{0.5}/4$	$2.028^{+0.448}_{-0.366}$
II/IV	15	0.99	1.065 ± 0.082	0.332	334^{+15}_{-14}	0.500	0.506 ± 0.022	$x/4$	$2.047^{+0.185}_{-0.170}$
III/IV	12	0.99	1.142 ± 0.122	0.261	559^{+24}_{-23}	0.707	$0.676^{+0.029}_{-0.028}$	$x^{0.5}/2$	$1.828^{+0.161}_{-0.149}$
IV/IV	23	–	(1.000)	(1.000)	762	1.000	(1.000)	$x/2$	(2.000)
V/IV	18	0.98	0.934 ± 0.089	2.235	963^{+35}_{-34}	1.414	$1.458^{+0.053}_{-0.051}$	$x^{0.5}$	$2.124^{+0.157}_{-0.147}$
VI/IV	9	0.99	1.065 ± 0.100	1.286	1208^{+58}_{-55}	2.000	$1.955^{+0.094}_{-0.090}$	x	$1.912^{+0.189}_{-0.172}$
VII/IV[f]	1	–	–	–	–	2.828	2.8 –	$2x^{0.5}$	1.9 –
Mars									
'B'/IV[f]	2	–	–	–	–	0.177	0.19 –	$x^{0.5}/8$	2.2 –
'A'/IV	3	0.99	1.12 ± 1.98	0.12	89^{+209}_{-63}	0.250	$0.24^{+0.55}_{-0.17}$	$x/8$	$1.8^{+7.9}_{-0.9}$
I/IV	10	0.99	1.010 ± 0.072	0.336	250 ± 12	0.354	0.360 ± 0.017	$x^{0.5}/4$	$2.068^{+0.209}_{-0.190}$
II/IV	16	0.99	1.013 ± 0.076	0.456	438^{+19}_{-18}	0.500	$0.496^{+0.021}_{-0.020}$	$x/4$	$1.967^{+0.169}_{-0.156}$
III/IV	18	0.99	1.055 ± 0.064	0.490	464^{+19}_{-18}	0.707	$0.699^{+0.028}_{-0.027}$	$x^{0.5}/2$	$1.953^{+0.161}_{-0.144}$
IV/IV	26	–	(1.000)	(1.000)	620	1.000	(1.000)	$x/2$	(2.000)
V/IV	14	0.99	0.978 ± 0.075	1.736	1047^{+49}_{-43}	1.414	$1.505^{+0.070}_{-0.061}$	$x^{0.5}$	$2.265^{+0.216}_{-0.180}$
VI/IV	13	0.99	1.016 ± 0.075	1.785	1313^{+73}_{-69}	2.000	$1.980^{+0.110}_{-0.104}$	x	$1.961^{+0.224}_{-0.200}$
VII/IV	10	0.98	0.924 ± 0.162	4.655	2462^{+271}_{-244}	2.828	$2.786^{+0.307}_{-0.276}$	$2x^{0.5}$	$1.941^{+0.451}_{-0.365}$

[a] Equations of form $Y = aX^b$, where Y = observed $D_{I...VII}$, X = observed D_{IV}, Y_c = calculated $D_{I...VII}$, and ± values of b are at the 95% confidence interval; values of Y_c and $\bar{X}_g$ are given here in the alog domain.

[b] Source: calculated by authors from data in Table I only; no two-ring basins or protobasins; provisional ranks 'A' and 'B' lie inside rank I. All regressions significant at 1% level.

[c] $\bar{X}_g$ = geometric mid-point of observed D_{IV} for each ring group.

[d] Expresses spacing between each equation and that for the main ring (IV/IV) in terms of adjacent $2^{0.5}$ groups, through a variable x raised to power of the constant 0.5.

[e] $x = (\text{alog } [\log(Y_c/\bar{X}_g) + (5-R) \log 2^{0.5}])^2$, where R = rank of rings for which Y_c is calculated; $\pm x$ values are at the 95% confidence interval; *model* x for *all* ring groups = 2.000 (Fielder, 1963).

[f] No least-squares fit; $Y_c/\bar{X}_g$ and x are geometric means or single values only.

(for $n \geq 5$) are shown in Figures 6b–8b, where the inverse correlation between sample size and dispersion of the $D_{\text{I-VII}}/D_{\text{IV}}$ data in each group of rings is clearly evident. Rings are not evenly distributed across all seven ranks, but range from 5 to 18 (excluding all ranks IV and rank VII on Mercury and the Moon). All ranks on the three planets are not equally robust. A few rings clearly fall between the better-defined trends, and in 14 instances two (in one case three) closely spaced ('split') rings from the same basin occupy a position normally filled by only one ring. Slopes of the 18 non-$D_{\text{IV}}/D_{\text{IV}}$ distributions in Table III range from 0.80 to 1.14, and average 1.00 ± 0.15 (n = 207 rings, statistics weighted by number of rings per $D_{\text{I-VII}}/D_{\text{IV}}$ distribution). The mean slope of unity was expected from past study of the dimensions of impact craters and other geometrically-similar landforms (Baldwin, 1963; Wilhelms *et al.*, 1977; Pike, 1982). All regressions in Table III are significant at the 1% confidence level ($n \geq 5$).

The spacing of multiple rings on the three planets, as derived specifically for grouped data, correspond to those predicted by the $2.0^{0.5}$D lunar model (Fielder, 1963). However, the agreement is not perfect, and the scatter evident within the ranked groups in Figures 6–8 precludes treating the $2^{0.5}$D increment as a 'law'. The statistics of the agreement are detailed in Tables III–V and summarized for basins and protobasins on several planets and satellites in Table VI.

Observed departures from the $2^{0.5}$D spacing that result from dispersion in the data for the ring groups are evaluated at the center of each least-squares fit. We do this by calculating the ratio $Y_c/\bar{X}_g$ and then measuring the width of the fitted 95% confidence interval at $\bar{X}_g$. Y_c is the point estimate of $D_{\text{I...VII}}$, here at $\bar{X}_g$; $\bar{X}_g$ is the geometric mid-point of D_{IV}, calculated separately for each $D_{\text{I...VII}}/D_{\text{IV}}$ ring group. Dispersion in the observations from the three planets is sufficiently low that both point *and* interval (error-bound) estimates of ring diameter from the regression analysis (Tables III, V) are statistically robust for most ranks (Figures 6b–8b). Analysis of covariance reveals that the parallel $D_{\text{I-VII}}/D_{\text{IV}}$ distributions differ significantly from their neighbors at the 1% level. However, only the point estimates of Y_c are satisfactory for some ranks constructed from a small sample (I and VII on the Moon and Mercury).

Departures of the observed $Y_c/\bar{X}_g$ (Table III, column 8) from the model ratio, defined as the closest fraction or integer multiple of $2.0^{0.5}$D (Table III, column 7), are minor. $Y_c/\bar{X}_g$ differs with ring rank, but deviations for all ranked ring diameters can be compared directly by expressing $Y_c/\bar{X}_g$ ratios in terms of a variable, x, that is raised to the constant power 0.5, such that model $x = 2.0$ (our convention; alternatively, x could be held constant and the exponent varied). To do this we equated each observed $Y_c/\bar{X}_g$ with an algebraic expression containing x (under 'Form', column 9 in Table III) so that the *model* spacing, *regardless of ring rank*, always is 2.0. Thus, similarity/difference of any ring rank to/from the hypothesized model is evident immediately by proximity of x (Tables III–V, last columns) to 2.0. For example, because $D_{\text{IV}}/D_{\text{IV}} = 1.0$, the expression required to make $x = 2.0$ is $x/2$. For $D_{\text{V}}/D_{\text{IV}}$, which the model predicts to be 1.414 (i.e. $2.0^{0.5}$), the

commensurate expression is $x^{0.5}$; the observed 1.505 value for the $Y_c/\bar{X}_g$ ratio of rings V/IV on Mars, for which $x = 2.3$, in Table III exceeds the hypothesized spacing.

We similarly analyzed pairs of adjacent-ring groups (Table IV) to eliminate bias introduced by correlation with rank IV. This alternative has the advantage of yielding x without the different algebraic conversions required in Table III (column 9), but it does not preserve the accompanying confidence interval. Instead, the standard deviation has been calculated for averaged x values in Table VI. The spacings in Table IV were derived from the results of least-squares regression in Table III: Values of x in Table IV were extracted from observed ratios of $(Y_c/\bar{X}_g)$ values for adjacent ring ranks in Table III. Comparison of results from the two analytic modes in Table VI shows them to be similar.

Values of x corresponding to the 22 non-D_{IV}/D_{IV} *measured* $Y_c/\bar{X}_g$ ratios of ring groups on the three planets vary from 1.8 to 2.4 in Table III and from 1.6 to 2.3 in Table IV. (Comparable terrestrial values are 1.8 to 2.1; Pike, 1985). Mean x for all three planets (Table III results) is $2.011 + 0.195, -0.176$, 95% C.I. The average departures of the observed x from 2.0 in Table III are roughly comparable for the Moon (0.012), Mercury (0.002), and Mars (0.019); values for Earth and the outer planet satellites, derived from fewer data, are expectedly high: 0.070 and 0.090, respectively.

Differences between observed $Y_c/\bar{X}_g$ and model ratios of basin rings are both systematic and nonsystematic. The latter are evident in the nonunity slopes of the least-squares fits in Table III and scatter of $D_{I\text{-}VII}/D_{IV}$ values above and below the lines, both for each planet and across all three bodies. We ascribe the nonsystematic variations to random causes of little genetic significance: small sample sizes, the

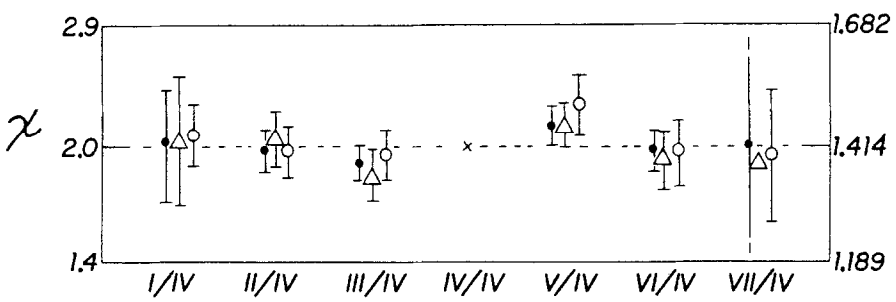

Fig. 9. Agreement of observed with model intervals of spacing for multi-ring basins, from correlation analysis of six ranked ring groups, on the Moon, Mercury, and Mars (Figures 6–8, data from Table III). Averaged spacings of observed ring groups cluster about model value ($\bar{x} = 2.0$), and avoid intervals between groups. Rings III and V lie farther from model value than other rings. Best fit to $2.0^{0.5}$D model is $x = 2.0$; worst fits are extreme values of x, 1.414 and 2.828, which are equivalent to distances midway between 'model' D_n/D_{IV} equations spaced exactly at $2.0^{0.5}$D intervals. Horizontal axis: Rank-grouped ring diameters paired in least-squares fits (except IV/IV). Vertical axis (left): Intervals of mean radial separation between $D_{I...VII}$ and D_{IV} observed for seven groups of basin rings on the Moon (dots), Mercury (triangles), and Mars (circles). Values of $\bar{x}$ and 95% C.I. (error bars) calculated in log domain (see Table III, footnote). Vertical axis (right): Raw-ratio equivalents of x for adjacent ring positions (cf. Figure 13).

TABLE IV

Spacing of adjacent basin rings, from linear least-squares fits to rings grouped by rank: multi-ring basins

Adjacent ring groups[a]	Combined n[b]	Ratio of observed $Y_c/\bar{X}_g$ for adjacent ranks[c]	Observed x[d]
		Moon	
'A', I	7	1.3	1.7
I, II	20	1.392	1.938
II, III	29	1.387	1.923
III, IV	32	1.453	2.111
IV, V	34	1.457	2.124
V, VI	25	1.362	1.854
VI, VII	12	1.4	2.1
		Mercury	
'A', I	9	1.5	2.2
I, II	22	1.421	2.019
II, III	27	1.336	1.786
III, IV	35	1.479	2.188
IV, V	41	1.458	2.124
V, VI	27	1.342	1.800
VI, VII	10	1.4	2.0
		Mars	
'B', 'A'	5	1.3	1.6
'A', I	13	1.53	2.33
I, II	26	1.379	1.903
II, III	34	1.409	1.985
III, IV	44	1.431	2.048
IV, V	40	1.505	2.265
V, VI	27	1.316	1.731
VI, VII	23	1.407	1.980

[a] From Table I; multi-ring basins only.
[b] See Table III.
[c] From results of least-squares fits and statistics of ring spacing in Table III; model value = 1.414.
[d] x for adjacent ranks = $(Y_c/\bar{X}_g)^2$; model value = 2.000 (Fielder, 1963).

degraded or otherwise nonoriginal state of many of the basins (including possible topographic reversal on Mars), and various random influences on the ring-forming process. We have identified no planet-specific differences in ring spacing from the data in Tables III and IV, thus confirming the findings of Wood and Head (1976) from a much smaller data set.

There is, however, a curious symmetry about the main ring on all three planets (first identified in Pike and Spudis, 1984b). Ring groups III and V both lie farther from ring IV, and commensurately closer to rings II and VI respectively, than the $2.0^{0.5}$D interval. Values of x in Table III range from 1.83 to 1.95 for rank III and from 2.12 to 2.27 for rank V. The displacement of rings III and V shows up even more clearly in the results for adjacent groups of paired rings in Table IV, which gives an explicit value for the narrow spacing between rings II and III and between rings V and VI (averaged $x = 1.853$, Table VI). This value is masked by the referenced-to-ring-IV technique (Table III).

Figures 6–8 show that the displacement of rings III and V can not have resulted from the few split rings in ranks III (2%) and V (8%). The effect, which was evident – albeit unnoticed at the time – for ring V in Figure 27 of Hartmann and Wood (1971), is weaker on the Moon than elsewhere, and it is particularly strong on Mercury. (Also evident on Mercury – but only slightly on Mars and absent on the Moon – is a tendency for ranks III and V to converge around IV with increasing basin size). This important second-order variation in ring spacing does not show up in the meager data thus far available for Earth and the outer-planet satellites.

Overall similarity in the geometry of grouped rings of multi-ring basins on Mars, Mercury, and the Moon enables all 296 rings (67 basins) to be combined into a general model for ring spacing on the terrestrial planets (Table VI; Figure 9). We have done this by computing means, standard deviations, and 95% confidence intervals of x (non-D_{IV}/D_{IV} values from Tables III and IV) for the three planets. Statistics for the combined model were weighted by the number of rings for each planet. The calculations are in two sets: Data for rings III and V, which have a slightly different spacing, are separated from those for the other four ranks. (The three values of x for rings III/IV are converted, by [4.0-x], to express their greater distance from ring IV in the same direction as values for V/IV, and thus not cancel out their larger absolute values).

The $2^{0.5}$D spacing constant proposed by Fielder (1963) for four lunar basins is at once both confirmed in a much wider application and modified. The results are summarized in Table VI: (1) ring groups ranked as I, II, VI, and VII are spaced from the main ring, rank IV, at average x increments of $(1.990 \pm 0.154)^{0.5}$D, C.I. = $+0.229$ -0.203, or their integer multiples; (2) grouped rings occupying positions III and V are spaced from ring IV at a larger average increment $(2.134 \pm 0.071)^{0.5}$D, C.I. = $+0.157$ -0.145. Interval estimates of x at two sigma (from the 95% C.I.), 1.781 to 2.219 and 1.989 to 2.291, respectively, overlap so much that the mean values of x seem to differ little. However, a t-test reveals that the means differ at any level of significance. Thus the slightly different geometry of rings III and V differs so *systematically* from that of other basin rings on all three bodies, that the spacing increment for grouped basin rings on the inner planets could be regarded as a compound, rather than a single, value.

5.1.2. *Alternate Ring Positions of Multi-Ring Basins*

The spacing interval between observed neighboring rings within individual basins commonly is about 0.5D (or 2.0D, by reversing order of the rings) rather than $2.0^{0.5}$D (Hartmann and Kuiper, 1962). This systematic difference is explained by the recognition, anticipated by Hartmann and Kuiper (1962, Table 2), that adjacent rings *mapped* for a basin do not always occupy adjacent ring *positions*, or ranks, in Figures 6–8. For example, the four rings identified at the Eitoku-Milton basin on Mercury (Spudis, 1984) fall into ranks, II, IV, V, and VI, but not III. However, the $2^{0.5}$D spacing still describes this basin, and the many analogous cases, because all its ring groups belong to *integer multiples* of $2^{0.5}$D. The D_{III} position simply is unoccupied, and the adjacent observed rings II and IV are spaced at a multiple or fraction of $2^{0.5}$D, such as 0.5D (Hartmann and Wood, 1971). The 'missing' ring III of Eitoku-Milton evidently did not form or has been buried or obliterated. Analogous 'missing' structural rings in terrestrial meteorite craters may not exist, or they may have formed but have not yet been recognized (Pike, 1985).

5.1.3. *Two-Ring Basins*

The rings of all double-ring basins *that lack central peaks* also are spaced at an interval of approximately 0.5D, not $2^{0.5}$D. According to this observation of Hartmann and Wood (1971) (see also Baldwin, 1963; Howard *et al.*, 1974; and Wood, 1980), which is elaborated in Pike (1985), the inner rings (D_i) are essentially similar to ring II of multi-ring structures. The resemblence in Figure 10 is supported by the least-squares results (Tables V, VI) from the observations in Table II. D and D_i on the Moon, Mercury, and Mars ($n = 53$) are spaced at an average x increment of $(1.948 \pm 0.022)^{0.5}$D, C.I. = $+0.112$ -0.104 (Table VI). Comparable figures for D_{II}/D_{IV} (averaged from Table III) are $(1.995 \pm 0.045)^{0.5}$D, C.I. = $+0.164$ -0.151 ($n = 46$). A t-test reveals that mean D_i/D and D_{II}/D_{IV}, while close, are not statistically similar at the 5% level of significance. Two-ring basins have slightly smaller inner rings.

From the discussion of alternate ring positions for multi-ring basins, in Section 5.1.2., it follows that the 0.5D spacing of two-ring basins in Figure 10 probably is a variant of the $2^{0.5}$D-spacing – characteristic of small basins only (Hartmann and Kuiper, 1962; Hartmann and Wood, 1971) – wherein a potential ring position always remains unfilled or a ring's structure is so subdued in amplitude as to be unrecognizable. Thus, the 0.5D-interval of two-ring basins almost certainly arose similarly to that of larger, multi-ring basins, and is not a separate spacing 'rule' that requires a different formational mechanism. More importantly, the similarity suggests no genetic difference between large and small basins save that of scale (Wood, 1980), a generalization that extends to protobasins (Pike, 1982; 1985), despite their quantitative difference in ring spacing, and large complex craters as well. We emphasize a final, and most important, implication of the close correlation between D_i/D and D_{II}/D_{IV} in Figure 10: The near similarity argues strongly against the 'intermediate' ring (rank III) of multi-ring basins being the main ring, an

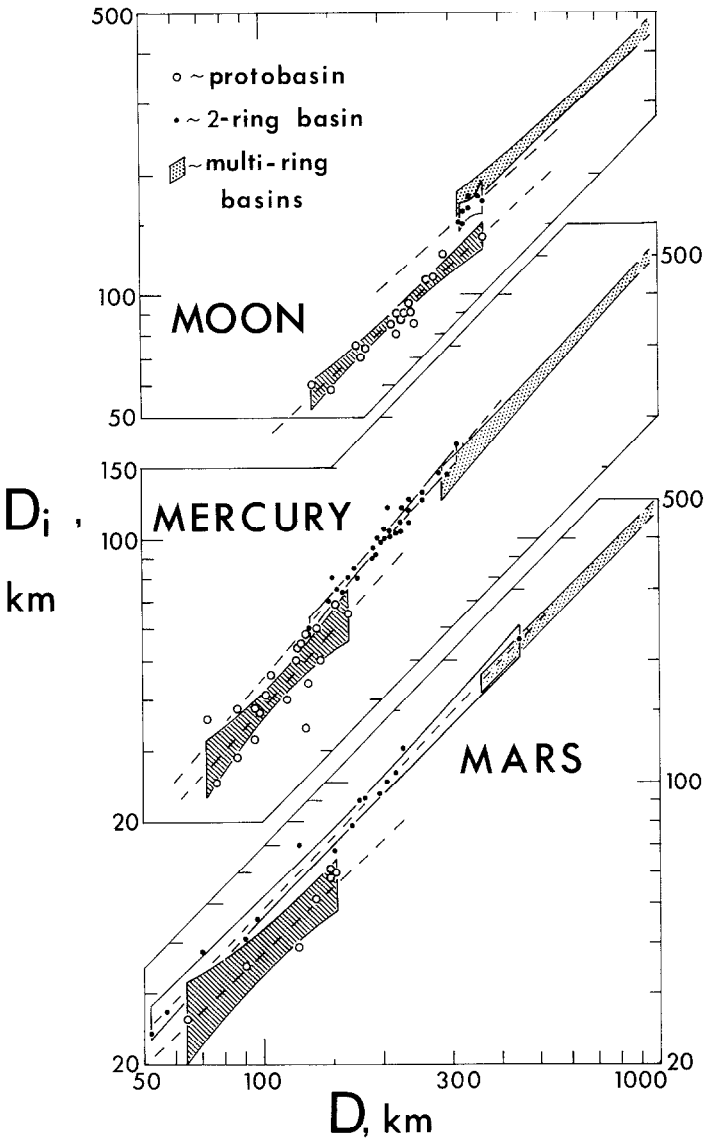

Fig. 10. Ring-diameter correlations for protobasins (circles) and two-ring basins (dots) on the Moon (n = 17, 7), Mercury (n = 20, 31), and Mars (n = 7, 15). Data (Table II) are values of inner ring diameter, D_i, as a function of main ring (rim) diameter, D. The nine paired curves enclose 95% confidence intervals for linear log-log fits to the three plots of protobasins (lower, shaded), the three plots of two-ring basins (unshaded), and to the three plots of rings II/IV for multi-ring basins (upper, shaded; see Figures 6b–8b). Six dashed lines are linear fits to the data (Table V). Ring geometry of two-ring basins is quite close to that of rings II/IV of multi-ring basins, but differs significantly (at the 1% confidence level) from that of protobasins.

TABLE V

Spacing between inner (D_i) and outer (D) rings, from linear least-squares fits to ring diameters[a]

Results of regression analysis[b]					Statistics of ring spacing			
D_i/D ring groups[c]	n	r	b, Slope	a, Y_c at $X=1$ km, km	$\bar{X}_g$[d]	Y_c, 95% C.I. at $\bar{X}_g$, km[d]	Observed $Y_c/\bar{X}_g$, 95% C.I.[e]	Observed x 95% C.I.[f]
Moon								
2-Ring basins	7	0.70	0.88 ± 1.04	1.005	342	165 ± 9	0.484 ± 0.026	$1.874^{+0.215}_{-0.196}$
Protobasins	17	0.96	0.913 ± 0.141	0.640	222	88 ± 3	$0.400^{+0.014}_{-0.013}$	$1.280^{+0.091}_{-0.082}$
Mercury								
2-Ring basins	31	0.98	1.130 ± 0.096	0.247	202	100 ± 2	0.494 ± 0.009	$1.952^{+0.074}_{-0.072}$
Protobasins	20	0.85	1.044 ± 0.378	0.316	109	42 ± 3	$0.387^{+0.030}_{-0.028}$	$1.198^{+0.194}_{-0.167}$
Mars								
2-Ring basins	15	0.99	1.018 ± 0.078	0.454	152	75 ± 3	$0.496^{+0.021}_{-0.020}$	$1.968^{+0.170}_{-0.155}$
Protobasins	7	0.95	0.920 ± 0.366	0.545	99	37 ± 5	$0.377^{+0.049}_{-0.043}$	$1.137^{+0.315}_{-0.245}$

[a] Source: calculated by authors from ring diameters in Table II only; no multi-ring basins; identical calculations (not shown here) carried out on same observations, but in D/D_i format, summarized in Table VI.

[b] Equations of form $Y = aX^b$, where Y = observed D_i, X = observed D, Y_c = calculated D_i, and $\pm$ values of b are at the 95% confidence interval; values of Y_c and $\bar{X}_g$ given here in the alog domain. All regressions except that for lunar 2-ring basins (5%) are significant at 1% level of confidence.

[c] Protobasins are large craters with an inner ring (D_i) and a central peak; 2-ring basins have no central peak.

[d] $\bar{X}_g$ = geometric mid-point of observed D for each subset of paired rings.

[e] Y_c calculated at $\bar{X}_g$; *model* $Y_c/\bar{X}_g$ for all subsets shown here = 0.500.

[f] $x = (\text{alog } [\log(Y_c/\bar{X}_g) + 3 \log 2^{0.5}])^2$, where $\pm x$ values are at the 95% confidence interval; *model* $\bar{x} = 2.000$ (Fielder, 1963).

equivalence that is a key element in some models of ring genesis (e.g., Head, 1974, 1977a).

5.1.4. *Protobasins*

The ring spacing in protobasins, two-ring structures *that also have central peaks*, clearly differs from that of peakless two-ring basins (Pike, 1982; 1985, Figure 3). The inner rings of protobasins are proportionally smaller. Protobasins have been regarded as small and morphologically immature peak-plus-inner-ring basins, but really are mature 'super-craters'. (It is no accident that Hartmann and Wood, 1971, initially termed them 'central-peak *craters*', not 'basins'). The difference in ring

spacing between protobasins and mature basins on all three planets is evident in our least-squares results (Figure 10, Tables V, VI) from the measurements in Table II. D and D_i of protobasins ($n = 44$) are spaced at an average x increment of only $(1.220 \pm 0.053)^{0.5}$D, C.I. at 95% = $+0.188$ -0.157, whereas comparable values for two-ring basins are virtually 2.0 (see discussion above and Tables III, V, and VI). Formal statistical tests comparing both D/D_i ratios and the regression equations show that protobasins differ significantly from two- and multi-ring basins (D_{IV}/D_{II}) at any level.

The morphometric contrast between protobasins and mature two-ring basins (Figure 10), which span the size-morphologic transition from the largest complex craters to the smallest multi-ring basins (Stuart-Alexander and Howard, 1970), can be explained by presence of the undersized central peak in protobasins: If a peak *and* an inner ring form in a crater, *each* is smaller than it would be if the other were absent (Hale and Grieve, 1982; Pike, 1983, 1985). Thus the mechanism(s) of ring formation within two-ring and multi-ring basins may apply equally to protobasins.

5.1.5. *Summary of Least-Squares Ring Groups*

The weighted mean value of x for the 32 non-D_{IV}/D_{IV} groups of basin rings on all bodies examined thus far, including Earth and three outer-planet satellites, is essentially 2.0: 1.998 ± 0.22 (Table VI). Adding the three groups of two-ring basins (Table V) does not alter these figures: 1.989 ± 0.20 C.I. (Table VI). The deviation of rings III and V about ring IV are so symmetric, when expressed in this form, that they sum to zero and hence do not affect $\bar{x}$. Thus the mean spacing increment observed for grouped basin rings, specifically when referenced to the main ring, varies within a fairly restricted range, from $1.8^{0.5}$D to $2.2^{0.5}$D, never far from $2.0^{0.5}$D. The 95% confidence interval lies well within one $2.0^{0.5}$D interval – the distance separating adjacent ring groups. However, comparable x values for the three groups of protobasins (Table V), 1.220 ± 0.16, are so unlike those for basins that the two sets of ring data differ significantly at any level. The disparity indicates that calculations including protobasins with two- and multi-ring basins can yield erroneous conclusions (cf. Wood and Head, 1976, Figure 14; Head, 1977, Figure 5).

5.2. Adjacent Rings of Individual Basins

The spacing of multiple rings can be examined basin-by-basin, if enough rings are present. In this section we present statistics of ring spacing for single multi-ring basins on Mars, Mercury, and the Moon (Pike, 1981; Clow and Pike, 1982). Two-ring basins and protobasins are necessarily excluded. Measurements of average ring diameters and their rank are from Table I. Analysis of ring rank:ring diameter for adjacent-ranked rings of individual basins yields an average spacing of $(2.01 \pm 0.26)^{0.5}$D, in substantial agreement with the results for rings in least-squares groups (Section 5.1).

We estimated a value of the spacing increment, x, for each basin from a functional dependence of log ring size (Y) upon radial ring position, or rank (X). This relation

was established by a linear least-squares fit for each basin, initially with three or more rings (total $n = 64$ basins, 278 rings): on the Moon ($n = 18, 85$), Mercury ($n = 22, 85$), and Mars ($n = 24, 108$). The equations, after Clow and Pike (1982) from Fielder (1963), are of the form $\log D_n = \log D_{IV} + (n\text{-}4) \log b$, where D_n is diameter of a ring of any rank n and D_{IV} is diameter of the main ring, both in km. Ring ranks are similarly spaced integers in arbitrary units, and $\log b$ is slope. Diameters for the correlations were weighted 1, 2, or 3, according to their quality (Table I). Figure 11 shows three examples of the observations and the resulting least-squares lines.

Fits of the equation to each basin yielded statistical estimates of the slope b and diameter of the main basin ring D_{IV}* (Table VII). The average spacing increment for adjacent (ranked) rings within a basin, x, is the square of alog slope, $(\text{alog } b)^2$. Rings III and V, which lie farther from ring IV than the nominal 2.0 spacing increment in grouped-data results, above, were not separated from those in other ranks in the analysis of individual basins. (Otherwise, the number of basins remaining with enough rings for the fits would have been too few.) We had anticipated that this forced inclusion of rings III and V (e.g., rings III and V of Al Qahira, Figure 11 and Table I) would yield fits with slopes uniformly greater than $2.0^{0.5}$. However, the average observed excess of slope over 2.000, 0.012, is so much smaller than the accompanying confidence interval that it is not statistically significant. Values of x for individual basins (Table VII) range from 1.913 (Grimaldi) to 2.241 (Balmer) on the Moon, from 1.800 (Bartok-Ives) to 2.282 (Shakespeare) on Mercury, and from 1.768 (Argyre) to 2.270 (Sirenum) on Mars.

Mean values of x for each planet lie close to the model spacing-increment of 2.000. However, the average dispersion of alog slope, b, given here by the mean 95% confidence interval (C.I.) around $\bar{x}$, is high: Moon, 2.034 + 0.323 − 0.299; Mercury, 2.006 + 0.667 − 0.579; and Mars, 2.004 + 0.523 − 0.449. We examined C.I. values as a function of the number of rings in each basin, and found an inverse, strongly nonlinear, dependency (Figure 12). The relation between sample size and dispersion of slope is approximately linear for basins with 4 to 7 rings, but three-ring

TABLE VI

Mean spacing increment, $\bar{x}$, for grouped basin rings analyzed by least squares[a]

Planet or satellite (and multi-ring groups)	Referenced to main ring (rank IV)			Adjacent ring ranks	
	Number of rings (no. IV)[b]	Number of ring groups[c]	$\bar{x}$ and 95% C.I.[d]	Combined n[e]	$\bar{x}$ and s[f]
Two rings (D_i/D): Moon + Mercury + Mars (Table V)					
2-ring basins	53/53	3	$1.946^{+0.120}_{-0.112}$[g]	106	1.946 ± 0.029
Protobasins	44/44	3	$1.220^{+0.173}_{-0.147}$[g]	88	1.220 ± 0.053

Planet or satellite (and multi-ring groups)	Referenced to main ring (rank IV)			Adjacent ring ranks	
	Number of rings (no. IV)[b]	Number of ring groups[c]	$\bar{x}$ and 95% C.I.[d]	Combined n[e]	$\bar{x}$ and s[f]
Three or more rings (Tables III, IV)					
Moon (all ring groups)	64/59	7	$2.012^{+0.151}_{-0.138}$	159	1.996 ± 0.120
Mercury (all groups)	64/61	7	$1.998^{+0.203}_{-0.182}$	171	2.015 ± 0.162
Mars (all groups)	86/81	8	$2.019^{+0.224}_{-0.197}$	212	2.020 ± 0.185
Earth (all groups)[h]	18/18	4	$1.93^{+0.37}_{-0.30}$	42	1.98 ± 0.12
Outer Satellites (all groups)[i]	19/14	6	$1.91^{+0.75}_{-0.50}$	44	1.96 ± 0.14
Moon + Mercury + Mars:					
(all ring groups)	214/201	22	$2.011^{+0.195}_{-0.176}$	542	2.011 ± 0.159
'Nominal' spacing:					
(no III/IV, V/IV)	122/109	10	$1.990^{+0.229}_{-0.203}$	–	–
('A'/I, I/II, VI/VII)	–	–	–	147	1.991 ± 0.154
'Wide' spacing:					
(III/IV, V/IV)	92/92	6	$2.134^{+0.157}_{-0.145}$	226	2.142 ± 0.071
'Close' spacing:					
(II/III, V/VI)	–	–	–	169	1.853 ± 0.089
Summary: Two- and multi-ring basins (above)					
Moon + Mercury + Mars:					
(all M – R groups + 2-ring basins)	267/254	25	$1.998^{+0.177}_{-0.160}$	648	2.000 ± 0.136
All bodies:					
(all multi-ring groups)	251/233	32	$1.998^{+0.243}_{-0.204}$	628	2.006 ± 0.155
(all M – R groups + 2-ring basins)	304/286	35	$1.989^{+0.218}_{-0.185}$	734	1.997 ± 0.135

[a] Source: Tables III–V; for derivation of x see Table III.

[b] Number of rings correlated with ring IV; first value $= n$ for $\bar{x}$; second value $= n$ for 95% C.I.

[c] Including one-ring groups; IV/IV excluded.

[d] Weighted by number of rings ($n \geq 5$) in each group.

[e] Summed numbers of rings in paired adjacent ranks (≥ 3 rings; Table IV); all rings (2 rings; Table V).

[f] Weighted by number of rings in each paired group (Tables IV, V).

[g] Respective values from identical calculations in D/D_i format are: $2.049^{+0.108}_{-0.102}$ and $3.433^{+0.478}_{-0.409}$.

[h] Pike (1985).

[i] R. J. Pike, unpublished preliminary ring diameters for basins on Rhea, Ganymede, and Tethys.

TABLE VII

Least-squares fits to basin-ring rank and diameter[a]

Basin[b]	Number of rings	r	D_{IV*} (km)	Slope, b	x, 95% C.I.[c]	
Moon						
Orientale	6	0.999	924	1.420	2.016	+0.103 −0.098
Imbrium	6	0.999	1137	1.427	2.036	+0.095 −0.091
Nectaris	5	0.994	871	1.403	1.967	+0.292 −0.225
Moscoviense	5	0.998	432	1.428	2.040	+0.196 −0.179
Mendel-Rydberg	4	0.999	428	1.458	2.126	+0.220 −0.199
Hertzsprung	4	0.992	548	1.419	2.013	+0.639 −0.485
Humorum	6	0.996	424	1.386	1.920	+0.166 −0.152
Smythii	5	0.999	760	1.431	2.047	+0.123 −0.116
Crisium	5	0.999	524	1.443	2.081	+0.111 −0.105
Grimaldi	3	0.995	432	1.383	1.913	+2.610 −1.104
Humboldtianum	6	0.996	684	1.420	2.016	+0.179 −0.164
Coulomb-Sarton	4	0.996	461	1.406	1.977	+0.420 −0.347
Serenitatis South	5	0.999	895	1.462	2.137	+0.111 −0.105
Korolev	4	0.999	429	1.388	1.927	+0.154 −0.143
Ingenii	4	0.999	320	1.412	1.994	+0.211 −0.191
Apollo	3	0.999	491	1.435	2.060	+0.935 −0.643
Balmer	3	0.999	393	1.497	2.241	+1.319 −0.831
Keeler-Heaviside	4	0.996	493	1.476	2.179	+0.521 −0.420
Mercury						
Borealis	3	0.997	1567	1.358	1.843	+1.519 −0.833
Gluck-Holbein	3	0.999	487	1.411	1.990	+0.929 −0.633
Sobkou	3	0.984	900	1.374	1.889	+6.100 −1.442
Brahms-Zola	4	0.999	609	1.362	1.854	+0.169 −0.155
Donne-Molière	4	0.999	1066	1.414	1.999	+0.113 −0.107
Hiroshige-Mahler	3	0.997	336	1.475	2.176	+2.265 −1.110
Mena-Theophanes	4	0.996	788	1.466	2.150	+0.504 −0.409
Tir	4	0.988	1333	1.482	2.198	+1.024 −0.699
Budh	3	0.997	827	1.407	1.979	+1.980 −0.990
Ibsen-Petrarch	4	0.994	624	1.430	2.044	+0.564 −0.442
Andal-Coleridge	5	0.986	1329	1.396	1.948	+0.440 −0.359
Matisse-Repin	4	0.999	857	1.448	2.096	+0.069 −0.067
Bartok-Ives	4	0.993	1125	1.341	1.800	+0.426 −0.345
Hawthorne-Riemenschneider	4	0.999	537	1.410	1.987	+0.155 −0.144
Vincente-Yakolev	4	0.992	710	1.412	1.993	+0.598 −0.460
Eitoku-Milton	4	0.999	1189	1.420	2.017	+0.088 −0.085
Sadi-Scopas	4	0.993	909	1.374	1.888	+0.469 −0.376
Tolstoy	4	0.993	499	1.439	2.072	+0.615 −0.474
Caloris	6	0.997	1330	1.438	2.067	+0.171 −0.158
Chong-Gauguin	4	0.992	900	1.407	1.979	+0.615 −0.469
Shakespeare	3	0.996	438	1.511	2.282	+3.512 −1.383
Van Eyck	4	0.995	286	1.372	1.884	+0.382 −0.317

Table VII (continued)

Basin[b]	Number of rings	r	D_{IV*} (km)	Slope, b	x, 95% C.I.[c]
			Mars		
Al Qahira	6	0.994	742	1.420	2.017 +0.221 −0.199
near Newcomb crater	4	0.996	853	1.459	2.129 +0.517 −0.416
Ladon	5	0.994	579	1.356	1.838 +0.234 −0.208
Chryse	5	0.999	1282	1.482	2.196 +0.174 −0.162
Mangala	3	0.988	694	1.442	2.080 +6.995 −1.603
Sirenum	4	0.992	497	1.507	2.270 +0.855 −0.621
so. of Hephaestus Fossae I	4	0.991	458	1.465	2.145 +0.766 −0.565
no. of Hephaestus Fossae II	3	0.996	1053	1.399	1.958 +2.174 −1.030
southeast of Hellas	3	0.996	535	1.398	1.954 +2.379 −1.073
south of Renaudot crater	4	0.999	651	1.446	2.090 +0.110 −0.104
south of Lyot crater	5	0.996	389	1.400	1.961 +0.228 −0.204
Cassini	5	0.998	444	1.452	2.108 +0.168 −0.155
Deuteronilus-B	4	0.999	194	1.451	2.105 +0.140 −0.131
Deuteronilus-A	5	0.997	207	1.370	1.876 +0.173 −0.158
near South crater	5	0.974	774	1.359	1.846 +0.555 −0.426
near Schiaparelli crater	5	0.993	428	1.434	2.056 +0.338 −0.291
near La Verrier crater	4	0.999	474	1.348	1.818 +0.093 −0.088
Noctis Labyrinthus	5	0.999	1851	1.451	2.105 +0.103 −0.098
South Polar	3	0.986	872	1.405	1.975 +6.770 −1.529
Argyre	6	0.996	803	1.330	1.768 +0.134 −0.124
Isidis	4	0.998	1451	1.422	2.022 +0.287 −0.252
Hellas	7	0.999	2252	1.378	1.898 +0.071 −0.069
Huygens	3	0.999	468	1.392	1.937 +0.571 −0.441
near Cassini	6	0.999	356	1.443	2.083 +0.103 −0.098
			Summary[d]		
Moon (15 basins)	73	–	–	1.424	2.029 +0.220 −0.192
Mercury (16 basins)	67	–	–	1.414	2.000 +0.394 −0.312
Mars (19 basins)	93	–	–	1.417	2.008 +0.260 −0.217

[a] From observations in Table I; values of D_{IV*} and b shown here in the alog domain; fits are of form log D_n = log D_{IV} + $(n - 4)$ log b, where D_n = ring diameter at any rank n, D_{IV} = diameter of main ring (both in km), and log b = slope. All regressions significant at 1% level.

[b] Many names are provisional, and do not constitute official nomenclature.

[c] x = (alog b)^2.

[d] Means weighted by number of rings (≥ 4).

basins have a dispersion about four times that expected from an extrapolation from basins with four or more rings. Thus diameter:rank fits to three-ring basins are too poorly constrained to yield robust estimates of the dispersion for slope of the equations (and hence basin-ring spacing). Accordingly, we deleted the 14 three-ring basins and recalculated mean slope and its dispersion for the remaining 50 basins (233 rings). The resulting values for $\bar{x}$ and mean C.I., weighted by number of rings per

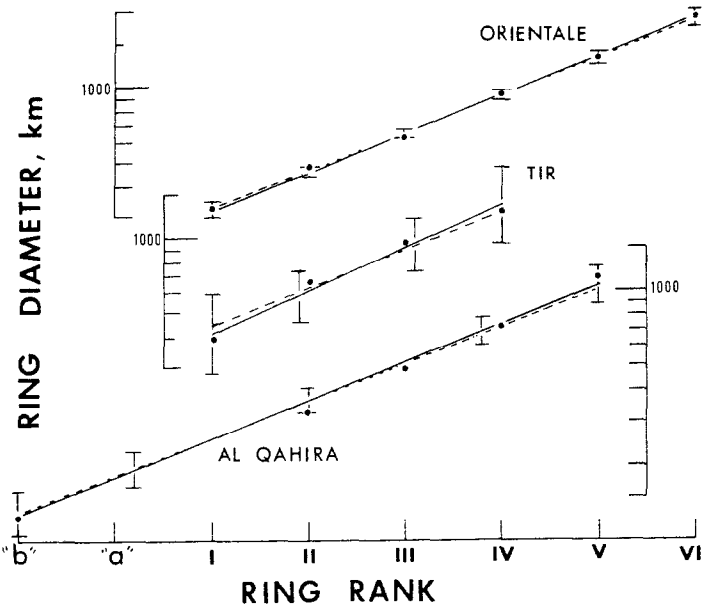

Fig. 11. Log ring diameter (dots) as a function of ring rank (arbitrary units) for the three basins shown in Figures 1–3 (Table VII): Orientale (Moon), Tir (Mercury), and Al Qahira (Mars). All data from Table I. Solid lines, linear least-squares fits of the form $\log D_n = \log D_{IV} + (n\text{-}4) \log b$ (Equation 4 of Fielder, 1963, recast by Clow and Pike, 1982), where n = any ring rank, D_{IV} = diameter of the main basin rim, and $\log b$ = slope. Ring diameters weighted by quality of observations (see text). Error bars define 95% confidence interval. Calculated slope, b, yields average spacing increment between adjacent rings of each basin. Dashed lines, spacing model, where $b = 1.4142$ ($\bar{x} = 2.000$). Observed values of b for the three basins are respectively, 1.420 O0.036 ($x = 2.016 \pm 0.101$), 1.482 $\pm$ 0.286 ($x = 2.198 \pm 0.862$) and 1.420 $\pm$ 0.074 ($x = 2.017 \pm 0.210$). Table VII gives results for the other 61 basins. Average x for each planet (Table X) lies close to the model value of 2.0.

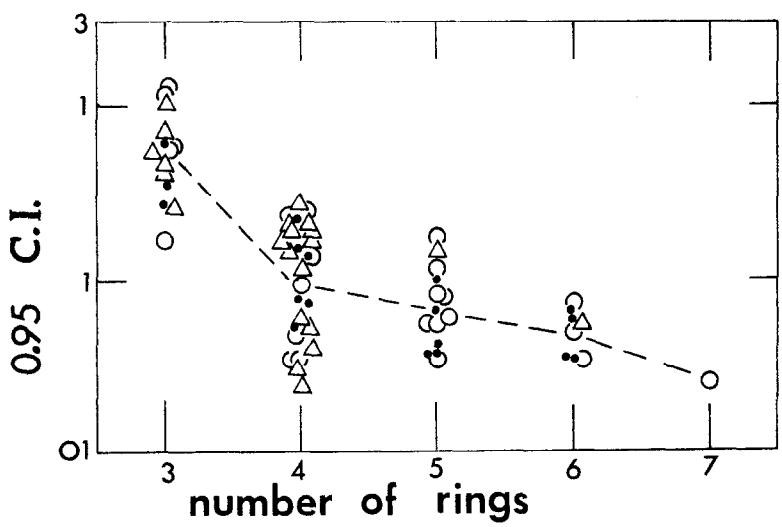

Fig. 12. Nonlinear inverse dependency of the 95% confidence interval, which shows dispersion of alog slope, b, for least-squares fits to multi-ring basin ring diameter and ring rank, upon number of rings per basin (Table VII). Diameter/ring fits to three-ring basins are poorly constrained. Dots: Moon, triangles: Mercury, circles: Mars. Dashes connect geometric means at 0.95 C.I.

basin, are (Table VII): Moon, 2.029 + 0.220 − 0.192 (n = 15 basins, 73 rings); Mercury, 2.000 + 0.394 − 0.312 (n = 16, 67); and Mars, 2.008 + 0.260 − 0.217 (n = 19, 93).

The revised average-spacing increments for single basins are barely changed from the initial ones. However, the values of dispersion are reduced substantially, and approach the intrinsically lower ones derived from analyses of grouped basins in Section 5.1 (Table VI). The weighted mean $\bar{x}$ and C.I. values for all three bodies from Table VII are 2.012 + 0.286 − 0.236. This observed 95%% C.I., 1.776 to 2.298, lies well within one $2.0^{0.5}$D interval, 1.414 to 2.829 (Defined by distances midway between log x model ring-spacing values 1.0, 1.414, 2.0, 2.828, etc.). Whether the observed mean 95% C.I. – although narrow – is small enough to differ significantly from one that might arise from random processes (cf. Clow and Pike, 1982) remains to be tested (as in the next section). However, this is unnecessary. A t-test for the correspondence of log b and log $2.0^{0.5}$ reveals no difference between the two, for all 50 basins, at the 1% level of significance. Thus, basin rings are spaced at $2.0^{0.5}$D intervals.

5.3. Ring-Diameter Ratios

Finally, we present an analysis of ratios of ring diameters, the first and most-commonly applied parameter of ring spacing (Hartmann and Kuiper, 1962; Fielder, 1963; Hartmann and Wood, 1971; Howard *et al.*, 1974; Wood and Head, 1976). Table VIII summarizes the scope of our observations for multi-ring basins from the average ring diameters of 67 basins in Table I. The basic data are 214 ratios of diameters of adjacent *observed* basin rings, D_n/D_{n-1} (where n is ring rank). The rings include both *adjacent ranked* and *alternate ranked* rings. The number of ratios for two-ring basins and protobasins, 97, is the same as the number of structures (Tables II, V).

5.3.1. *Multi-Ring Basins*

First, we examine multi-ring basins (Figure 13). The 214 ratios fall into the two clusters of values found by Hartmann and Kuiper (1962) for multi-ring and double-ring basins on the Moon: The first cluster, centered at about 1.4 to 1.5, usually describes adjacent ranks (n = 169); the second, centered at about 2.0, usually is for alternate ranks (n = 45). Data on the second cluster are sparse (three of the 45 ratios span more than one basin-ring rank and hence are omitted from further calculations). To supplement the few observed alternate-rank ratios we generated a second set of 103 'alternate ring-rank' ratios by deliberately skipping one *observed* ring in calculating each ratio (Table VIII, Figure 13). Additionally, the three subsets of ratios were grouped according to inclusion or exclusion of rings III or V, established in Section 5.1 to be systematically displaced. The total number of possible subsets for multi-ring basins (Table IX) is 30, six of which are not subdivided according to rings III and V.

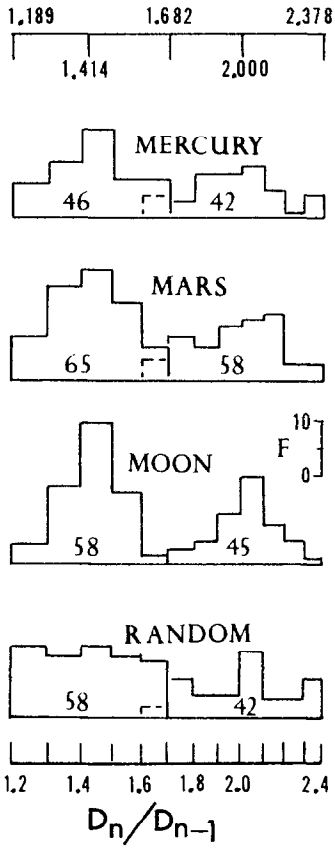

Fig. 13. Ratios of diameters (D) of *observed adjacent* rings for multi-ring basins on the three planets (larger D/smaller D, from Table I). Most of the 314 observed ratios fall into two groups (Table IX): those for *adjacent ranked* rings (histograms on left, $n = 169$; cf. Figure 9) and those for *alternate* ranked rings (historgrams on right, $n = 145$). (Three ratios skip > 1 ring and are omitted here). Most ratios in each group lie wholly within one of two $2^{0.5}$D intervals (cf. Figure 9): either 1.189 to 1.682 or 1.682 to 2.378 (upper scale), and cluster around the respective spacing-model values of 1.414 for adjacent ranked rings and 2.000 for alternative ranked rings ($x = 2.0$ in both cases). Two frequency distributions of ratios were drawn at random (RAND Corp., 1955) for the same two $2^{0.5}$D intervals, 1.189 to 1.681 and 1.682 to 2.378, to statistically test the groups of observed ratios for nonrandomness (see text and Table IX). (Dispersion of the $n = 42$ sample is identical to that of the other, despite the 'peak' at $D_n/D_{n-1} = 2.05$).

Mean and standard deviation were calculated, in the log (D_n/D_{n-1}) domain (basin-ring ratios also are skewed strongly toward high values), for each of the 21 groups of observed ratios for multi-ring basins (Table IX). We judged that nine other groups had too few (< 10) ratios for stable statistics. For subsequent tests, the same two statistics were calculated for two sets of ratios drawn from a standard table of random numbers (RAND Corp., 1955), one set ($n = 58$) corresponding to ring ratios for adjacent ranks (1.189 t0 1.682), the other ($n = 42$) to ratios for alternate ranks (1.682 to 2.378). (The intervals are defined by distances midway between two log

TABLE VIII

Numbers of multi-ring basins, ring diameters, and their ratios[a]

Planet	Multi-ring basins	Rings as mapped	Ring positions ranked	Ratios: rings in adjacent ranks[b]	Ratios: rings in alternate ranks	
					No observed ring skipped[b]	One observed ring skipped[b]
Moon	18	85	82	58	6	39
Mercury	23	92	87	46	18	24
Mars	26	119	112	65	21	40
Totals	67	296	281	169	45[c]	103

[a] Raw data from Table I.
[b] See Table X.
[c] Three ratios omitted (see text).

D_n/D_{n-1}) model ring-spacing values, respectively 1.0, 1.414, and 2.0 and 1.414, 2.0, and 2.828). We transformed all statistics of D_n/D_{n-1}) to the domain of the spacing increment, x, so that (1) statistics for both adjacent and alternate ranks are directly comparable (Table IX), and (2) the results are comparable with those from sections 5.1 and 5.2. Calculations were weighted 1 to 5 by combining weights assigned to individual rings in Table I.

The 267 observed ratios (x equivalents) in the 21 *multi*-ring basin categories where $n > 10$ (Table IX) cluster around the model spacing increment of 2.000. The combined weighted mean for all three planets is $2.039 + 0.382 - 0.284$, close to the values obtained above both for least-squares groups and for ranked rings of individual basins. The net excess of observed x over model $\bar{x}$, $+ 0.040$, lies well within the accompanying error bounds. It is statistically insignificant. Weighted mean values for individual planets, excluding subsets 'All' (multi-ring plus two-ring basins) and those with < 10 ratios in Table IX, are $2.091 + 0.248 - 0.221$ (Moon, $n = 82$ ratios); $1.997 + 0.319 - 0,274$ (Mercury, $n = 67$); and $2.027 + 0.393 - 0.333$ (Mars, $n = 118$).

Differences in mean spacing among 'close', 'wide', and 'neither close nor wide' ring ratios, although not tested for significance, are strong enough to show up clearly in averaged x values of these groups in Table IX: respectively $1.928 + 0.353 - 0.305$ ($n = 62$ ratios), $2.117 + 0.304 - 0.265$ ($n = 92$), and $1.976 + 0.314 - 0.270$ ($n = 91$). The mean spacing for ring ratios V/III is, expectedly, much larger than 2.0: $\bar{x} = 2.287 + 0.441 - 0.364$ ($n = 22$), because *both* rings are spaced abnormally far from ring IV.

TABLE IX

Ratios of ring diameters: Statistics of central tendency and dispersion for basins and protobasins[a]

Groups of *ring ratios*[d] (outer/inner)	Mean, ± standard deviation[b], (number of ratios) [results for raw ratios below, and their x equivalents above[c]]		
	Moon	Mercury	Mars
	Adjacent ring ranks		
All (ignoring rank and sample size, n)	2.082 +0.243 −0.218 (58)[e] [1.443 +0.082 −0.078]	2.085 +0.390 −0.328 (46) [1.444 +0.129 −0.119]	2.056 +0.392 −0.329 (65) [1.434 +0.131 −0.120]
II/I, VII/VI (spacing neither wide nor close)	– (8)[f] –	– (4)[f] –	2.017 +0.383 −0.323 (14) [1.420 +0.129 −0.119]
III/II, VI/V close spacing)	1.995 +0.256 −0.225 (20)[e] [1.412 +0.088 −0.082]	1.888 +0.352 −0.297 (12) [1.374 +0.123 −0.133]	1.929 +0.412 −0.371 (19) [1.389 +0.141 −0.128]
IV/III, V/IV (wide spacing)	2.116 +0.224 −0.204 (30)[e] [1.455 +0.075 −0.072]	2.097 +0.327 −0.283 (30)[e] [1.448 +0.109 −0.101]	2.138 +0.356 −0.306 (32)[e] [1.462 +0.117 −0.109]
Randomly-chosen values from 1.189 to 1.682	←	2.069 +0.475 −0.387 (105) [1.438 +0.157 −0.141]	→

Table IX (continued)

Groups of ring ratios[d] (outer/inner)	Mean, ± standard deviation[b], (number of ratios) [results for raw ratios below, and their x equivalents above[c]]		
	Moon	Mercury	Mars
	Alternate ring ranks: No observed ring skipped[h]		
All (ignoring rank, n) but protobasins	1.930 +0.338 −0.288 (13) [1.965 +0.165 −0.152]	1.973 +0.337 −0.288 (49)[e] [1.986 +0.163 −0.151]	1.893 +0.387 −0.321 (33) [1.946 +0.190 −0.173]
IV/II, VI/IV (spacing neither wide nor close)	− (6)[f] −	1.961 +0.339 −0.288 (13) [1.981 +0.164 −0.152]	1.887 +0.352 −0.297 (13) [1.943 +0.174 −0.159]
III/I, VII/V (close spacing)	− (0)[f] −	− (5)[f] −	− (5)[f] −
D/D_1 for two-ring basins[g]	2.126 +0.218 −0.195 (7)[e] [2.062 +0.103 −0.097]	2.054 +0.241 −0.216 (31)[e] [2.027 +0.116 −0.109]	2.033 +0.302 −0.263 (15)[e] [2.107 +0.144 −0.135]
D/D_1 for protobasins[j]	3.143 +0.429 −0.309 (17)[i] [2.507 +0.166 −0.155]	3.294 +1.155 −0.855 (20)[i] [2.567 +0.416 −0.358]	3.410 +0.661 −0.553 (7)[i] [2.612 +0.242 −0.211]
Randomly-chosen values from 1.682 to 2.378	←	2.020 +0.460 −0.375 (42) [2.010 +0.217 −0.196]	→

Table IX (continued)

Groups of ring ratios[d] (outer/inner)	Mean, ± standard deviation[b], (number of ratios) [results for raw ratios below, and their x equivalents above[c]]		
	Moon	Mercury	Mars
	Alternate ring ranks: One observed ring skipped		
IV/II, VI/IV (spacing neither wide nor close)	2.044 +0.240 −0.214 (20)[e] [2.022 +0.115 −0.109]	1.897 +0.237 −0.211 (12)[e] [1.948 +0.118 −0.111]	1.997 +0.345 −0.294 (19) [1.999 +0.166 −0.153]
III/I, VII/V (close spacing)	− (7)[f] −	− (3)[f] −	1.849 +0.421 −0.342 (11) [1.923 +0.208 −0.188]
Rings V/III (doubly wide spacing)	2.263 +0.306 −0.269 (12)[e] [2.127 +0.139 −0.131]	− (9)[f] −	2.316 +0.603 −0.478 (10) [2.152 +0.264 −0.235]
	Summary (adjacent + alternate ring ranks)[k]		
All (ignoring rank, n) but protobasins	2.049 +0.34 −0.29 (74)	2.027 +0.39 −0.33 (95)	2.001 +0.39 −0.33 (98)

[a] Source: calculated by authors from data in Tables I, II.
[b] Calculations in log domain; ratios weighted 1 to 5 according to quality of data (see text).
[c] $x = (Y_c/\bar{X}_g)^2$ for adjacent ring ranks, and $(Y_c/\bar{X}_g)^2/2$ for alternate ring ranks and for two-ring basins and protobasins.
[d] Include ratios formed from a few rings ranked below I ('A', 'B').
[e] Dispersion of observed ratios is significantly less than that of ratios selected randomly within one $2^{0.5}$ interval, according to one-sided F-test carried out in the log x domain at the 5% level of significance.
[f] Too few data for stable statistics ($n \leq 9$), except protobasins.
[g] D equivalent to ring IV, D_i to ring II; protobasins have a central peak in addition to the inner ring.
[h] 'Doubly-wide' spacings (rings V/III) not observed (Ring IV intervenes).
[i] Mean D/D_i values for protobasins differ significantly from those for two-ring basins, by a 2-sided normal test carried out in the log domain at the 5% level of significance.
[j] Values for the six confirmed lunar protobasins (see Table II): 3.110 +0.451 −0.223 (6)[i]
[2.494 +0.175 −0.163].
[k] x equivalents only: standard deviations are estimates; no F-tests.

5.3.2. *Two-Ring Structures*

The 97 ratios for two-ring basins and protobasins fall into two clusters (Figure 14). One, for two-ring basins, is the Hartmann-Kuiper (1962) group (same as that for alternate ranks of multi-ring basins) centered at a D_n/D_{n-1} of about 2.0. The other, for protobasins, is recognized here for the first time. It is centered at about 2.5 D_n/D_{n-1}.

The 53 ratios (x equivalents) for the three two-ring basin categories (Table IX) cluster around the model spacing increment of 2.000. The combined weighted mean for all three planets is $2.058 + 0.258 - 0.229$, close to the values found above for ranked ring groups, single basins, and basin ring ratios. The close geometric correspondence, which bears out results obtained above from least-squares analysis of ring diameters (Table V), suggests that two-ring basins differ from their multi-ring counterparts only in size and number of rings.

The 44 ratios (x equivalents) for the three protobasin categories (Table IX) do not cluster around the model spacing increment of $D_n/D_{n-1} = 2.000$. Rather, the combined weighted mean for all three planets is $3.253 + 0.787 - 0.625$, quite unlike our values obtained for least-squares groups, ranked rings of individual basins, and ring ratios of two- and multi-ring basins. The disparity indicates that protobasins differ from larger basins in geometry. In fact, the difference between ring ratios for protobasins and both two- and multi-ring basins is statistically significant (by a two-sided normal test) at the 1% level. The result supports that obtained above from least-squares analysis of ring diameters (Table V) and the accompanying two implications for protobasins (Sections 5.1.4 and 5.1.5).

5.3.3. *Statistical Tests*

The observed average values of x for two- and multi-ring basins, although close to 2.0, support the spacing model only when a second condition is met: Dispersion about the mean must occupy limits too narrow to have occurred by chance. This requirement is necessary because $\bar{x}$ for randomly chosen ratios within one $2.0^{0.5}$ interval *also* is 2.0 (Table IX). Accordingly, we compared, by an F-test at the 5% level of significance (Natrella, 1963), the standard deviation, s, of each subset in Table IX with a value of s from one of the two sets of randomly generated ratios mentioned above. Calculations were carried out in the log (D_n/D_{n-1}) domain. Table IX has 23 testable subsets: Those 10 with ≤ 9 ratios and the three for protobasins were excluded.

All-in-all, the spread of observed basin-ring ratios about the mean *is* significantly less than that for the randomly drawn ratios, i.e., dispersion that might arise from random processes. This difference, with qualifications noted below, indicates that the $2.0^{0.5}$D ring spacing is real.

Results of the F-test are systematic, by ring-sample composition, by ring-sample size, and by planet (Table IX). The $2.1^{0.5}$D spacing of ring ranks III and V, although differing little from the $2^{0.5}$D of other rings, greatly affects test results. For the six subsets that mix rings of *all* ranks, the observed dispersion is significantly less than

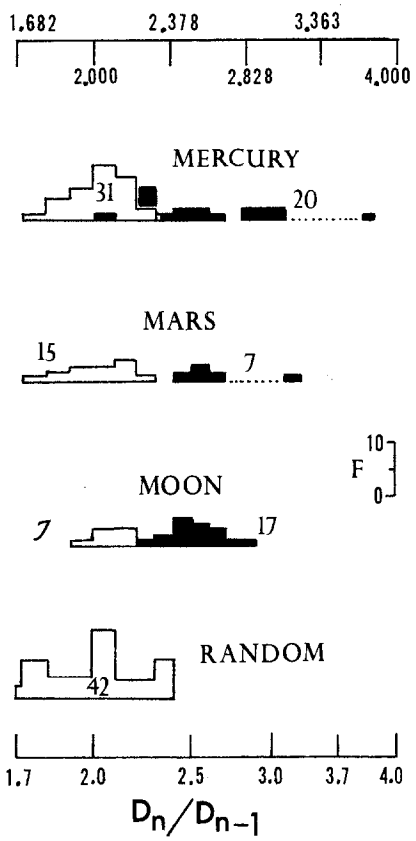

Fig. 14. Ratios of diameters (D) of paired rings for two-ring basins and protobasins on the three planets (D/D_i from Table II). The 97 ratios fall into two groups (Table IX): those for two-ring basins (open histograms, on left, $n = 53$) and those for protobasins (filled histograms, on right, $n = 44$). Ratios for two-ring basins lie wholly within the same $2^{0.5}$D interval, 1.682 to 2.378, occupied by alternate ranks of multi-ring bains (cf. Figure 9, 13), and cluster around the spacing-model value of 2.000 for alternate ranked rings ($\bar{x} = 2.0$). Ratios for protobasins do not occupy a $2^{0.5}$D interval that is related to the spacing of two- or multi-ring basins, but rather cluster around a value of ca. 2.6 ($\bar{x} = 3.3$) that is unique to protobasins and differs significantly from those for two- and multi-ring basins (Table IX). Random distribution is that in Figure 13.

random dispersion (i.e., a 'pass') for *only* two. However, for the 17 subsets that are constituted according to presence/absence of multi-ring ranks III and V or contain only two-ring basins, 9 pass. The effect of mixing ring ranks is so marked that F-test results omitting these six subsets are included (in brackets) for comparison, below.

Test results are highly sensitive to sample size. Of the 11 [6] subsets having ≥ 20 ratios, including two that describe two-ring basins, the observed dispersion is significantly less than random dispersion in eight [all 6] cases. Of the 12 [11] subsets containing ≤ 19 ratios, only three [3] pass. Clearly, when the sample is sufficiently large, dispersion of observed ring ratios is significantly less than that ascribed to chance. Most subsets 'failing' the F-test simply are too small – so small that their

difference from random is 'not proven' rather than 'disproven' a critical distinction suggesting that given adequate basin-ring observations, any subset could pass.

Planet-specific effects on our *F*-test results may include overall geologic history, efficacy of surface processes, and quality of spacecraft images. Five [5] out of six [5] subsets of lunar ring ratios pass the test; four [3] of the seven [5] Mercurian subsets pass; only two [1] of the 10 [8] Martian subsets (one of them, at $n = 32$, the largest subset tested) pass(es). We conclude that the $2.0^{0.5}$D spacing is strongest on the Moon, where basin rings are best exposed and most closely studied; weakest on Mars, where most rings are severely degraded and poorly exposed; and intermediate (but still much weaker than on the Moon) on Mercury, where degradation is slow but where the rings are not now well displayed, and may never have been strongly developed.

In sum, ratios excluding rings ranked III and V, but including two-ring basins, have a mean *spacing increment* ($\bar{x}$) of about 2.0 (Table IX). Corresponding *raw* ratios are approximately either 1.4 or 2.0. Ratios including rings ranked III and V, as for the least-squares groups described in Section 5.1, have a larger increment, x

TABLE X

Summary statistics for ring spacing: Moon, Mercury, Mars

Analytic method and ring groups	Mean spacing increment $\bar{x}$, 95% confidence interval
Least-Squares Groups of Ranked Rings[a]:	
All multi-ring groups + two-ring basins	$1.998^{+0.177}_{-0.160}$
Protobasins (D/D_i)	$3.433^{+0.478}_{-0.409}$
Diameter: Rank Correlated for Single Basins[b]:	
All multi-ring basins with ≥ 4 rings	$2.012^{+0.286}_{-0.236}$
Ratios of Ring Diameters[c]:	
All two- and multi-ring basins[d]	$2.024^{+0.38}_{-0.32}$
Protobasins (D/D_i)	$3.253^{+0.787}_{-0.625}$
Generalized Ring Observations for Inner Planets:	
All two- and multi-ring basins[e]	$2.01^{+0.28}_{-0.24}$
Protobasins[e]	$3.34^{+0.63}_{-0.52}$
Lunar basin ring-spacing model of Fielder (1963)	2.00

[a] Weighted means in Table VI. (D/D_i calculations for protobasins not shown).
[b] Weighted mean of three summary results in Table VII.
[c] Weighted means of two sets of results (three values each) in Table IX.
[d] Standard deviations are unweighted means of estimates.
[e] Unweighted means of, respectively, three and two results listed above.

TABLE XI

Contrasting models for basin rings

Models	Group A	Group B	Group C
Summary	Deep-seated structural changes during modification stage: 'Megaterracing'.	Impact-driven wave mechanism at penetration or excavation stage; Dominantly surficial	Differences in target strength or thickness; Syn- or post impact.
Proponents	McCauley, 1968 Hartmann and Wood, 1971 Head, 1974, 1977 Howard *et al.*, 1974 Mackin, 1969	Boon and Albritton, 1936 Baldwin, 1963, 1974, 1981 Van Dorn, 1968, 1969 Chadderton *et al.*, 1969 Murray, 1980 Pike, 1981	Fielder, 1963 Melosh and McKinnon, 1978 Hodges and Wilhelms, 1978 Wilhelms *et al.*, 1977 McKinnon, 1981
	← Grieve *et al.*, 1981 Croft, 1981b →		
Arguments for	(1) Terrestrial geologic evidence for structure associated with rings.	(1) Evidence for oscillatory uplift at terrestrial craters.	(1) Evidence for strength-related excavation at Ries.
	(2) Gravity-driven collapse likely at complex craters.	(2) Potentially explains the $2.^{0.5}$D spacing.	(2) Potential effects of lithospheric thickness hitherto underestimated.
Arguments against	(1) Does not explain $2^{0.5}$D spacing *or* outer rings.	(1) Physical plausibility remains uncertain.	(1) Does not explain $2^{0.5}$D spacing *or* outer rings.
	(2) Cannot form innermost rings unless they are part of excavation cavity.	(2) Evidence for deep structures associated with basin rings.	(2) Strength differences probably negligible at basin-scale impacts.

averaging 2.1. The *F*-test indicates, with 95% confidence, that these spacings did not arise by chance. Finally, ring spacing for the 44 protobasins, weighted x averaging 3.3 ± 0.6, C.I. at 95%, differs from both of the latter spacings significantly.

5.4. Summary of Ring Spacing

We have demonstrated that basin-ring spacing is nonrandom. Three different analyses of a large data set, much of it new, yield similar results on three terrestrial planets, regardless of their crustal structure and composition: One spacing increment dominates the ring geometry of two- and multi-ring basins. The spacing is the same both inside and outside the main basin ring. Exterior rings, once thought to be rare, are shown here to be nearly as common as interior rings. Protobasins have an entirely different ring spacing, commensurate with their morphologic immaturity and the presence of a small craterlike central peak.

Our summary descriptive model is as follows: Basin rings excluding ranks III and V, which immediately flank the main ring (IV), are spaced at an average increment, $\bar{x}$, of $(2.0 \pm 0.3)^{0.5}$D. Rings of two-ring basins are spaced at exactly twice this interval. Ranks III and V are separated from ring IV by an average increment of $(2.1 \pm 0.3)^{0.5}$D. (Error bounds are at 95% confidence interval). Thus the observed spacing of most basin rings is found to average $(1.7$ to $2.3)^{0.5}$D, and in two restricted cases $(1.8$ to $2.4)^{0.5}$D. Ring spacing effectively straddles the $2.0^{0.5}$D value proposed initially from data for a few lunar bsins by Fielder (1963). Rings of protobasins are spaced at a much larger mean x increment, 3.3 ± 0.6. Table X summarizes averaged values of mean spacing for grouped rings (Section 5.1), individual basins (Section 5.2), and ring ratios (Section 5.3) on the Moon, Mercury, and Mars. Within the conservative error limits applied here, the results are remarkably consistent.

6. Explaining Basin Rings

We think that the spacing of paired and multiple rings is sufficiently constant to impose some limits on formational hypotheses for impact basins and protobasins. The evidence assembled here, for many structures on three quite different geologic bodies, enables speculations on ring genesis to proceed from a firmer observational foundation. Ring-forming hypotheses fall into at least three groups (Table XI): structural, wave-form, and target-strength. Because the ring problem has been linked to that of basin excavation, these three models, in turn, are related to two classes of hypotheses for basin excavation (Table XII): proportional and non-proportional growth of the transient cavity.

6.1. Models independent of the $2^{0.5}$D spacing

The possibility of a constant $2.0^{0.5}$D spacing has not strongly influenced most explanations of basin rings listed in Table XI. Rather, the problem of basin-ring origin has been linked closely with that of basin excavation (Table XII), specifically the nature of the transient-crater rim (Wilhelms, 1984). Although neither size nor shape of the transient cavity is known, proponents of basin models frequently have attempted to identify a specific basin ring (usually of what we now call rank II, III, or IV) as the topographic rim of the excavation cavity.

In general, those workers favoring a small initial cavity (Table XII: Group A Models) have tended to appeal to structural origins for ring systems (Table XI: Group A), whereas those preferring a large cavity (Table XII: Group B) have held that physical properties of the target were responsible for rings (Table XI: Group C). The two classes of ring mechanisms are not mutually exclusive, and some hypotheses incorporate features of both. Perhaps the most comprehensive scheme is that of Grieve *et al.* (1981), who also included aspects of a third group of ring-forming hypotheses, the 'fluidization' model (Table XI: Group B). We now examine some examples of each of the three categories of ring models in Table XI.

The first approach is structural. The concept of a 'megaterrace', a large concentric

TABLE XII

Contrasting models of basin excavation

Model	Group A	Group B
Summary	Proportional growth of excavation cavity. Basins are scaled-up versions of smaller impact craters.	Non-proportional cavity growth. Basins form by at least some fundamentally different mechanisms than do small craters
Proponents	Gault, 1974 Croft, 1980, 1981, 1985 Grieve *et al.*, 1981 Schultz *et al.*, 1981 Spudis *et al.*, 1984 Spudis, 1986	Baldwin, 1963, 1974, 1981 Hodges and Wilhelms, 1978 Murray, 1980 Wilhelms, 1984, 1986 Schultz and Gault, 1986
Arguments for	(1) Predicts excavated depths and volumes that agree with lunar sample data	(1) Predicts shallow excavation cavity, in agreement with lunar sample data
	(2) Does not invoke hypothetical and untestable physical mechanisms	(2) Explains basin inner rings by either strength differences or oscillatory uplift and collapse
Arguments against	(1) Experiments indicate flow fields might change with increasing crater size	(1) Cratering process changes in some unknown way above certain energy level (*deus ex machina*)
	(2) Does not explain basin rings, let alone the $2^{0.5}$D spacing	(2) Does not explain basin *outer* rings

slump feature surrounding an initially smaller excavated crater (Table XI: Group A), was one of the earliest ideas to be advanced for the origin of basin rings on the Moon (Mackin, 1969; Gault, 1974; Head, 1974; Dence, 1976, 1977; McCauley, 1977; Melosh and McKinnon, 1978; and Croft, 1981b). The structural hypothesis is based in part on purportedly analogous rim failure evident in smaller lunar and terrestrial complex craters (Dence, 1964; Quaide *et al.*, 1965), although it has yet to be shown that such modest slumping can be scaled directly to basin-sized events. The basin workers above all agreed on a megaterrace origin for the outer ring(s) of basins, although not necessarily for all the rings shown here. Gault (1974) and Dence (1976, 1977) envisioned this mechanism forming all outer rings around a small, proportional-growth transient cavity. Those authors who equated the intermediate ring (usually our rank III) with the transient basin cavity suggested a dual mechanism whereby the outer ring was produced by megaterracing, but the inner rings formed by rebound, analogous to the central peaks of lunar craters (Head, 1974; McCauley, 1977; Scott *et al.*, 1978).

A completely different approach was taken by Baldwin (1963, 1974), after Boon and Albritton (1936), and then by Murray (1980). They argued that a basin-size impact would 'fluidize' the lunar crust in the target region, and that traveling waves would produce concentric rings like the ripples in a pond after a stone has been dropped into it (Table XI, Group B). The term 'fluidization' is used here in the sense that target materials behave like a fluid (Melosh, 1979); it does not imply any volatile content of the target as it does for the terrestrial process of fluidization. Baldwin (1963; 1974) suggested that lunar 'rock-tsunami' waveforms, propagated outward by the collision of a basin-forming projectile, would freeze in place as concentric raised rings. Murray (1980) elaborated Baldwin's (1974) idea of an oscillatory mechanism, whereby 'fluidized' lunar crust would produce ring systems by continuous back-and-forth overthrust of ripples until the deformed crust increased in strength and solidified, preserving the multi-ring pattern (see also Wilhelms, 1984).

The third approach appeals to target rheology, thickness, and gross structure. Hodges and Wilhelms (1978) and Wilhelms *et al.* (1977) advocated a nested-crater mechanism for basins whereby interior rings formed from intersection of global compositional layers in the lunar crust by the shock wave (Table XI, Group C). Each successively smaller basin ring represents the boundary of a crater of excavation in the next-deeper crustal layer, and the basin topographic rim marks the boundary of excavation of the largest, outermost crater. The existence of outer rings, which was questioned in the nested-crater model, was ascribed to structural deformation outside the transient-cavity rim (Wilhelms *et al.*, 1977). Melosh and McKinnon (1978) and McKinnon (1981) applied a theoretical approach to ring genesis in which they equated ring spacing with lithospheric thickness and rheology. The resulting model invokes a variable ring spacing, rather than the $2^{0.5}$D interval, on both inner planets and outer satellites. This 'ring-tectonic hypothesis' explains only rings inside the topographic rim.

We do not think that any of these models completely explains the several evenly spaced rings of large impact basins, particularly those outside the main ring, although some specific elements of each hypothesis may be valid. We especially question the dogma – generally, and hitherto uncritically, accepted – that one of the *observed* basin rings somehow must equate with the rim of the transient or excavation cavity. There simply is no evidence for this assumed, but very convenient, equivalence, nor is it required to effectively model the formation of multi-ring basins.

6.2. New constraints on origin

Our observations impose limits on any model of basin ring location and emplacement (Table XIII). Analytical results for the Moon, Mercury, and Mars indicate that: (1) basins may have up to seven concentric rings or ring positions; (2) the spacing of rings is not random, but rather has a fairly constant interval; (3) this interval prevails both inside and outside the main ring; (4) the interval lies at or close to $2^{0.5}$ (Table X); and thus (5) the process responsible for locating basin rings is spatially discrete rather than continuous.

The suggestion that basin rings are spaced at $2^{0.5}$D is not new (Fielder, 1963; Hartmann and Wood, 1971). What we have confirmed here is that this spacing factor prevails in over 100 basins on three different planets (cf. Wood and Head, 1976), not on the Moon alone, or specifically at Orientale. Each of the three planets has a unique geologic history, thermal evolution, and possibly bombardment history. By contrast, the similar spacing of rings despite interplanetary differences in targets poses difficulties for basin-ring models that require specially defined target layering (Hodges and Wilhelms, 1978) or planetary thermal conditions (Van Dorn, 1968; Melosh and McKinnon, 1978).

We have found that the spacing of basin rings is constant both within (rings I–III) and outside (rings V–VII) the main topographic rim (ring IV). This important result indicates that basin rings form – or at least that their locations are determined – penecontemporaneously with the basin-forming impact. It does not preclude subsequent modification of ring morphology by either passive or active processes. Similar spacing inside and outside the main ring merely suggests that (1) rings in both locales probably formed by the same processes and perhaps at the same time, and (2) the structural pattern of basin rings was already established before ring-modification processes operated.

Our results indicate that planetary target conditions may have only *second-order* effects on basin-ring topography. The constant spacing factor of about $2^{0.5}$D applies to basins of such widely varying geologic age and target rheology that, again, the basic structural pattern of basin ring formation must have been established at the time of the impact and in association with it.

The fact that all ring positions *predicted* for a given basin are not filled does not preclude one model spacing, because the rings that are observed are spaced at multiples of $2^{0.5}$D. The absence of a ring at any predicted position within a basin may be a consequence of several factors, including: (1) burial of low-relief ring topography by subsequent and thick geologic units, (2) erasure of created rings by either internal or external processes, and (3) unique target conditions that prevented the formation of a ring at the time of impact.

6.3. Previous Models Dependent on $2^{0.5}$D Spacing

Two principal explanations have been proposed for the constant mean spacing of about $2^{0.5}$D for rings on the Moon (Hartmann and Wood, 1971, p. 59), and for those now described on Mercury and Mars (Table X; Pike and Spudis, 1984). The mechanisms differ in every way: One appeals to post-impact concentric fracturing of a basin-interior margin that has been loaded statically by volcanic fill; it belongs tentatively to Group C in Table XI. The other entails propagation of a 'rock tsunami' outward through a planetary crust at impact (Table XI, Group B).

Fielder (1963, p. 1259), Hartmann and Wood (1971), p. 57–59), and Schultz (1976, p. 8 and 34) all have suggested that patterns of shear stress observed by Lance and Onat (1962) in experimentally deformed steel plates might explain the $2^{0.5}$D value for lunar rings. Rigidly supported plates 5″ and 10″ in diameter were loaded

hydrostatically, and the resulting radial and spiral stress patterns compared with those predicted from solution to the theory of rigid/plastic bending of circular plates. No shear strain was observed. Lance and Onat verified a predicted circumferential zone of transition between two contrasting stress regimes situated at 0.73R from the center of the plate. This distance lies well within our error bounds for the nominal spacing increment of basin rings (0.71R $\pm$ 0.11R, from Table X).

Five problems attend the proposed mechanism. First, and fatally, the oft-quoted '... concentration of fractures at 0.73R ...' described by Hartmann and Wood (1971, Figure 36) simply does not exist. Close reading of Lance and Onat (1962) reveals instead that the '... concentration of shear fractures resembling those found in a steel specimen under pure bending'. (Hartmann and Wood, 1971, p. 57) is located '... *near the support of the* (rigidly clamped) *plate*'. (Lance and Onat, 1962, p. 310); i.e., *at radial distance R, not 0.73R.*

The remaining problems are worth mentioning, for even without a fatal flaw, Lance–Onat deformation is unworkable for impact basins: The second problem is that the rigidly held plate, which is an essential condition for the 0.73R interface of stress patterns, is a particularly poor analog of the crustal configuration in and around a multi-ring basin. Third, the stress fields generated by Lance–Onat deformation require hydrostatic loading of the central basin region. Such loading undoubtedly occurs in deeply flooded or otherwise modified basins on the Moon (e.g. the mascon in Imbrium). However, the observation that fresh, little-flooded, and relatively unmodified lunar basins (e.g. Orientale) and also terrestrial multi-ring craters (Pike, 1985) – none of which are loaded in this way – display the same ring spacing argues against pure Lance–Onat deformation. Fourth, Lance–Onat fracturing specifically generates only *one* circumferential feature. A preposterously complex, multisequence history of repeated loading (e.g., Fielder, 1963) would be required for each basin to explain the multiple-ring pattern observed on all the planets and satellites. Finally, the lone circular pattern purportedly formed by the Lance–Onat mechanism would lie *within* the basin topographic rim; we have shown here that rings and arcs spaced at the $2^{0.5}$ increment are common *outside* ring IV.

The spacing of *several* rings at about $2^{0.5}$D has suggested to other authors, correctly we think, that the physical processes controlling ring locus and perhaps formation must be periodic (Van Dorn, 1968; 1969). The 'tsunami' mechanism of ring formation discussed above in its pure form (Baldwin, 1974) is analogous to water waves propagating from a point-source disturbance. As such, each successive ring is separated by the *same* distance from the ring immediately within it. This problem was recognized by Van Dorn (1968). He attemped to reconcile the tsunami model with the observed increasing-outward spacing on the Moon by invoking *ad hoc* a 50 km thick layer of loosely compacted debris overlying a rigid basement.

We find the most obvious drawback to such a wave model to be the requirement for a similar crustal structure at each basin-impact site on all three planets. The possibility seems vanishingly small. Another unrealistic attribute of the tsumani model is the dominantly surficial character of its resulting ring topography. Rather,

geologic studies have accumulated considerable evidence for deep structural deformation associated with basin rings (Hartmann and Wood, 1971; Schultz, 1976; McCauley, 1977). Finally, we find implausible the notion that elements of a *traveling* wave form would always 'freeze' at a similar and discrete ($2^{0.5}$D) interval (see also, Chadderton *et al.*, 1969, p. 261). Instead, a variety of spacings would be expected as the outward-propagating wave 'froze' at different distances from the impact focus at different basins.

A possible solution to problems with existing wave models invokes *standing* (or 'stationary'), rather than traveling waves. First, a standing wave pattern can have an increasing-outward spacing of adjacent rings. Second, a standing wave is more consistent with the discrete interval observed between basin rings than is a traveling wave. Chadderton *et al.* (1969) attempted to explain the $2^{0.5}$ spacing of Orientale basin rings as the result of standing waves produced by free-body vibrations of the entire Moon.

Although we think that adaptation of the standing-wave mechanism was an important development, this specific model has several difficulties. Perhaps most damaging is the observation that multi-ring basins occupy the same, continuous, geometric sequence as smaller two-ring basins (Pike, 1983, 1985). The smaller impacts, which produced basins a third the size of Orientale, (to say nothing of the even smaller ones on Earth), almost certainly carry too little energy to induce the whole-planet vibrations required to form rings. Moreover, standing-wave vibration requires a wave guide, in this case a resonant cavity, to set up constructive interference. Such a cavity must be available on all planets and at each basin site. Its geometry must be everywhere the same to produce the similar ring spacing observed at each basin.

6.4. Speculations on a Ring-Forming Mechanism

That some part of the basin itself might provide the resonant cavity is suggested by the radially symmetric pattern of damage to structures in the Mexico City earthquake of 19 September 1985 (Flores *et al.*, 1987). Overall damage was disposed in alternating, similarly spaced annuli of heavy and light destruction, but only within a local region of water-saturated sediments. The concentric zonation indicates that seismic longitudinal (p) waves reflected internally within the low-strength region (the resonant cavity), interfered with each other, and generated standing waves. Both maxima and minima of standing-wave solutions to the Poisson equation correspond spatially to the large surface accelerations, according to the geophysical model by Flores *et al.* (1987). Many areas of greatest damage from the 19 September 1985 earthquake are located in these concentric zones of maximal acceleration.

We find remarkable the several parallels between this terrestrial seismic event and ringed impact basins. They include: (1) an initiating disturbance of high energy and short duration; (2) a compact low-strength region enclosed by rigid materials; (3) concentric zoning at the surface; (4) a similar spacing of concentric elements. These similarities raise several issues: Might a large impact generate longitudinal waves that

interfere and create a ring-locating resonance within the low-strength ('fluidized'?) target bounded by high-strength planetary crust? Could ring positions thus determined also develop outside the low-strength center? What part of the basin might serve as the resonant cavity? The answers to such questions undoubtedly will be more complicated than a simple appeal to resonance of the reflected shock wave within a basin's 'strength cavity' (e.g., Pike and Spudis, 1984b). Although clearly intriguing, this new analog requires much further investigation before it can be developed into a plausible model for basin-ring spacing.

7. Discussion

A model for concentric rings (Table XIII) must be consistent with existing evidence and constraints on basin formation as well as those developed here. Accordingly, it should have at least the following attributes: (1) the basic impact mechanics are similar overall to those forming smaller craters, differing mostly in the total energy input; (2) ring spacing develops independently of gravity, location within a basin, and conditions of target or projectile; (3) the ring-locating processes invoked accommodate discrete ring positions, of which seven are now known; (4) the model accounts for the many associations of deep-seated geologic structure with topographic rings; (5) ring *location* is imprinted at the time of impact, and special circumstances at most only modify this early- established concentric pattern; (6) ring topography may not have formed by the same process(es) that determined ring position; and (7) ring location and emplacement of ring topography need not be coeval. Other constraints are summarized in Table XIII.

The average $2.0^{0.5}$D spacing of basin rings almost certainly was established at impact, although this characteristic precludes neither modulation of ring geometry by target inhomogeneities nor postimpact geologic changes in basin topography. However, we assert that these complicating factors modify ring morphology much more than ring position, and account for only some of the scatter evident in the statistics of dispersion for mean ring spacing. Among target effects that may modulate basin-ring morphology are pre-impact structure and topography (Head, 1977b), broad-scale crustal layering (Hodges and Wilhelms, 1978), and lithospheric thickness (Melosh and McKinnon, 1978). Post-impact changes are mainly volcanic and tectonic. Annular zones of structural weakness formed during basin excavation, which could persist long after the initial impact, may remain loci of later endogenic modification (Schultz, 1979; Schultz and Glicken, 1979; Schultz *et al.*, 1982).

We attribute split basin rings to the increasing influence of local crustal structure on ring morphology, but not necessarily position, with distance outward. First, split-ring morphology frequently coincides with weak topography outside the main ring: rings are increasingly scarce in ranks V to VII, and tend to be fragmented partial arcs where they occur (Table I). That such rings also occupy discrete $2^{0.5}$D-spaced positions is consistent with a decay in energy at greater distances (Chadderton *et al.*, 1969). We propose that these weaker ring-forming disruptions were more easily

TABLE XIII

Proposed synthesis of basin-ring origin

Constraints on Excavation

(1) Most lunar basin ejecta from crust; little evidence for mantle material.
(2) Excavated volume at Orientale = 4 to 8 × 10^6 km^3 (gravity, photogeology).
(3) Pre-basin structures preserved *within* main rim (Orientale, Imbrium).
(4) Basin impact melts (LKFM) are more mafic than composition of surface rocks.

Constraints on ring formation

(1) Main rim (rank IV) equivalent to rims of smaller (complex) craters.
(2) Many outer rings exist; age relation of their topography to basin unsure.
(3) Inner and outer basin rings on 3 planets are spaced at $2.^{0.5}$D intervals.
(4) Deep-seated structures are associated with basin rings.

Toward a model of basin and ring formation

(1) Proportional growth of cavity is valid: $D_{tc} = (0.5 \pm 0.1)$D, km.
(2) Maximum depth of excavation = $(0.1 \pm 0.02)D_{tc}$, km.
(3) Volume of ejecta for Orientale = 7.7 × 10^6 km^3.
(4) Basin impact melts are generated at crustal depths of 30 to 60 km (LKFM).
(5) Main rim forms by collapse around gravity-scaled excavation cavity.
(6) Ring *positions* (not necessarily topography) determined during impact.
(7) Ring locations and ring topography may not reflect same process(es).
(8) Ring loci due to wave phenomenon, possibly oscillation or resonance effect.
(9) Outer rings of largest impacts may arise from lithospheric fracturing

modulated by layering and other crustal inhomogeneities (e.g., Hodges and Wilhelms, 1978), thus frequently creating conditions favorable for the development of split rings.

The systematic displacement of ranks III and V from the main ring (Figures 6–8) is less readily explained. We suspect that the symmetry about ring IV is related to its topographic prominence (which suggests that most of our choices for the main ring were correct). Undoubtedly, the symmetry is a clue to physical processes operating during basin formation, perhaps 'shedding' of rings III and V from IV during oscillatory movements of the sort envisioned by Baldwin (1974) and Murray (1980). We have no explanation for the diameter-dependent convergence of ranks III and V for basins on Mercury (Figure 7b).

A tentative model for concentric rings that emerges from the constraints summarized here (Table XIII) resembles none of the existing hypotheses (Tables XI, XII) in pure form. Rather, it embodies elements of several models. We think prevailing evidence favors a proportional-growth transient cavity about half the diameter of the final main ring, which forms by collapse around a gravity-scaled excavation cavity no deeper than about 0.1 its diameter. Up to seven major ring positions spaced at $2^{0.5}$D are determined early during the excavation stage. We think this imprinting occurs through a wave mechanism that operates in an oscillatory or

resonant mode and can establish ring loci in both low- (fluidized?) and high-strength (unfluidized) target material (Melosh, 1979). The topography of inner rings may form at this time by the same mechanism. The topography of some, or even many, outer ring and arcs, particularly those of the largest impacts, may be emplaced post-impact, likely as the result of faulting at the loci determined early in the impact.

The synthesis outlined here represents only a first attempt on the problem of basin genesis from an analysis of basin rings. It still leaves unanswered some important questions about concentric-ringed structures on the planets. Perhaps the most intriguing of all is why rings are spaced at $2^{0.5}$D rather than at some other number.

Acknowledgements

RJP dedicates this paper to the memory of N. J. Tamamian, late of the U.S. Geological Survey. We thank Larry Soderblom, Gene Shoemaker, and Fred Hörz for helpful reviews. Chuck Wood and Jay Melosh commented on an earlier draft. We also appreciate advice on statistics from Gary Clow and Alex Woronow, and thank Joe Boyce of NASA's Planetary Geology Program for funding the work.

References

Baldwin, R. B.: 1949, *The Face of the Moon*, Univ. Chicago Press, pp. 38–47 and 200–216.

Baldwin, R. B.: 1963, *The Measure of the Moon*, Univ. Chicago Press, pp. 314–332.

Baldwin, R. B.: 1974, 'On the Origin of the Mare Basins', *Proc. Lunar Sci. Conf. 5th*, 1–10.

Baldwin, R. B.: 1981, 'On the Tsunami Theory of the Origin of Multi-ring Basins, in *Multi-ring Basins, Proc. Lunar Planet. Sci.* **12A**, pp. 275–288.

Boon, J. D. and Albritton, C. C.: 1936, 'Meteorite Craters and Their Possible Relationship to "Cryptovolcanic Structures"', *Field and Lab.* **5**, 1–9.

Carr, M. H. (ed.): 1984, *The Geology of the Terrestrial Planets*, NASA Spec. Publ. 469, 1984.

Chadderton, L. T., Krajenbrink, F. G., Katz, R., and Poveda, A.: 1969, 'Standing Waves on the Moon', *Nature* **223**, 259–263.

Clow, G. D. and Pike, R. J.: 1982, 'Statistical Test of the $\sqrt{2}$ Spacing Rule for Basin Rings', *Lunar Planet. Sci.* **XIII** 123–124.

Croft, S. K.: 1979, 'Impact Craters from Centimeters to Megameters', *Ph.D. dissertation*, Univ. of Calif. Los Angeles, 264 pp.

Croft, S. K.: 1980, 'Cratering Flow Fields: Implications for the Excavation and Transient Expansion Stages of Crater Formation', *Proc. Lunar Planet. Sci.* **11**, 2347–2378.

Croft, S. K.: 1981a, 'The Modification Stage of Basin Formation: Conditions of Ring Formation', in *Multi-ring Basins, Proc. Lunar Planet. Sci.* **12A**, pp. 227–257.

Croft, S. K.: 1981b, 'The Excavation Stage of Basin Formation: A Qualitative Model', in *Multi-ring Basins, Proc. Lunar Planet. Sci.* **12A**, pp. 207–225.

Croft, S. K.: 1985, 'The Scaling of Complex Craters', *Proc. Lunar Planet. Sci. Conf. 15, J. Geophys. Res.* **90**, C828–C842.

Davies, M. E., Dwornik, S. E., Gault, D. E., and Strom, R. G.: 1976, *Atlas of Mercury* (photographic edition), NASA Special Publ. 423.

DeHon, R. A.: 1978, 'In Search of Ancient Astro*problems*: Mercury', *Repts. Planetary Geology Program 1977-1978*, NASA Tech. Memo. 79729, pp. 150–152.

DeHon, R. A., Scott, D. H., and Underwood, J. R., Jr.: 1981, *Geologic map of the Kuiper quadrangle of Mercury* U.S. Geol. Survey Misc. Inves. Map I–1233, scale 1:5 000 000.

Dence, M. R.: 1964, 'A Comparative Structural and Petrographic Study of Probable Canadian Meteorite Craters', *Meteoritics* **2**, 249–270.

Dence, M. R.: 1976, 'Notes Toward an Impact Model for the Imbrium Basin', *Interdisciplinary Studies by the Imbrium Consortium* **1**, 147–155.

Dence, M. R.: 1977, 'The Contribution of Major Impact Processes to Lunar Crustal Evolution', *Phil. Trans. R. Soc. London* **A285**, 259–265.

Dietz, R. S.: 1946, 'The Meteorite Impact Origin of the Moon's Surface Features', *J. Geology* **54**, 359–375.

El-Baz, F.: 1972, 'Al-Khwarizmi: A New-found Basin on the Lunar Far Side', *Science* **180**, 1173–1176.

Fielder, G.: 1963, 'Nature of the Lunar Maria', *Nature* **198**, 1256–1260.

Floran, R. J. and Dence, M. R.: 1976, 'Morphology of the Manicouagan Ring-Structure, Quebec, and Some Comparisons with Lunar Basins and Craters', *Proc. Lunar Sci. Conf. 7th*, 2845–2865.

Flores, J., Novaro, O., and Seligman, T. H.: 1987, 'Possible Resonance Effect in the Distribution of Earthquake Damage in Mexico City', *Nature* **326**, 783–785.

Frey, H. and Lowry, B. L.: 1979, 'Large Impact Basins on Mercury and Relative Crater Production Rates', *Proc. Lunar Planet Sci. Conf. 10th*, 2669–2687.

Gault, D. E.: 1974, 'Impact Cratering', in R. Greeley and P. Schultz (eds.), *A Primer in Lunar Geology*, NASA Tech. Memo. X-62359, pp. 137–175.

Grieve, R. A. F., Robertson, P. B., and Dence, M. R.: 1981, 'Constraints on the Formation of Ring Impact Structures, Based on Terrestrial Data', in *Multi-ring Basins, Proc. Lunar Planet. Sci.* **12A**, pp. 37–57.

Hale, W. S. and Grieve, R. A. F.: 1982, 'Volumetric Analysis of Complex Lunar Craters: Implications for Basin Ring Formation', *J. Geophys. Res.* **87**, Suppl. A65–A76.

Hartmann, W. K.: 1981, 'Discovery of Multi-ring Basins: Gestalt Perception in Planetary Science', in *Multi-ring Basins, Proc. Lun. Planet. Sci.* **12A**, pp. 79–90.

Hartmann, W. K. and Kuiper, G. P.: 1962, 'Concentric Structures Surrounding Lunar Basins', *Commun. Lunar Planet. Lab.* **1**, 55–66.

Hartmann, W. K. and Wood, C. A.: 1971, 'Moon: Origin and Evolution of Multi-ring Basins', *The Moon* **3**, 3–78.

Head, J. W.: 1974, 'Orientale Multi-ringed Basin Interior and Implications for the Petrogenesis of Lunar Highland Samples, *The Moon* **11**, 327–356.

Head, J. W.: 1977a, 'Origin of Outer Rings in Lunar Multi-ringed Basins: Evidence from Morphology and Ring Spacing', in D. J. Roddy, R. O. Pepin, and R. B. Merrill (eds.), *Impact and Explosion Cratering*, Pergamon Press, New York, pp. 563–573.

Head, J. W.: 1977b, 'Regional Distribution of Imbrium Basin Deposits: Relationship to Pre-Imbrian Topography and Mode of Emplacement', in *Interdisciplinary Studies by the Imbrium Consortium*, Lunar Planet. Inst. Contrib. No. 268D, pp. 120–125.

Hodges, C. A. and Wilhelms, D. E.: 1978, 'Formation of Lunar Basin Rings', *Icarus* **34**, 294–323.

Howard, K. A., Wilhelms, D. E., and Scott, D. H.: 1974, 'Lunar Basin Formation and Highland Stratigraphy', *Rev. Geophys. Space Phys.* **12**, 309–327.

Ivanov, B. A.: 1976, 'The Effect of Gravity on Crater Formation: Thickness of Ejecta and Concentric Basins', *Proc. Lunar Sci. Conf. 7th*, 2947–2965.

Lance, R. H. and Onat, E. T.: 'A Comparison of Experiments and Theory in the Plastic Bending of Circular Plates', *J. Mech. Phys. Solids* **10**, 301–311.

Mackin, J. H.: 1969, 'Origin of Lunar Maria', *Bull. Geol. Soc. America* **80**, 735–748.

McCauley, J. F.: 1968, 'Geologic Results from the Lunar Precursor Probes', *American Inst. Aeronaut. Astronaut. J.* **6**, 1991–1996.

McCauley, J. F.: 1977, 'Orientale and Caloris', *Phys. Earth Planet. Interiors* **15**, 220–230.

McKinnon, W. B.: 1981, 'Application of Ring Tectonic Theory to Mercury and other Solar System Bodies', in *Multi-ring Basins, Proc. Lunar Planet. Sci.* **12A**, pp. 259–273.

McKinnon, W. B. and Melosh, H. J.: 1980, 'Evolution of Planetary Lithospheres: Evidence from Multiringed Structures on Ganymede and Callisto', *Icarus* **44**, 454–471.

Melosh, H. J.: 1979, 'Acoustic Fluidization: A New Geologic Process?', *J. Geophys. Res.* **84**, 7513–7520.

Melosh, H. J. and McKinnon, W. B.: 1978, 'The Mechanics of Ringed Basin Formation', *Geophys. Res. Letts.* **5**, 985–988.

Moore, H. J., Hodges, C. A., and Scott, D. H.: 1974, 'Multiringed Basins – Illustrated by Orientale and Associated Features', *Proc. Lunar Sci. Conf. 5th*, 71–100.

Moore, J. M., Spudis, P. D., Pike, R. J., and Greeley, R.: 1984, 'Multiringed Basins of the Saturnian Satellites', *Geol. Soc. America Abstracts With Programs* **16,** 600.

Murray, B. C., Belton, M. J. S., Danielson, G. E., Davies, M. E., Gault, D. E., Hapke, B., O'Leary, B., Strom, R. G., Suomi, V., and Trask, N.: 1974, 'Mercury's Surface: Preliminary Description and Interpretation from Mariner 10 Pictures', *Science* **185,** 169–179.

Murray, J. B.: 1980, 'Oscillating Peak Model of Basin and Crater Formation', *Moon and Planets* **22,** 269–291.

Natrella, M. G.: 1963, *Experimental Statistics*, Natl. Bureau Standards Handbook 91, pp. 4–1 to 4–14.

Oberbeck, V. R.: 1975, 'The Role of Ballistic Erosion and Sedimentation in Lunar Stratigraphy', *Rev. Geophys. Space Phys.* **13,** 337–362.

Pike, R. J.: 1981, 'A Size: Rank Model for Basin Rings', *Repts. Planetary Geology Program – 1981*, NASA Tech. Memo. 84211, 123–125.

Pike, R. J.: 1982, 'Crater Peaks to Basin Rings: The Transition on Mercury and other Bodies', *Repts. Planetary Geology Program –1982*, NASA Tech. Memo. 85127, 117–119.

Pike, R. J.: 1983, 'Large Craters or Small Basins on the Moon', *Lunar Planet. Sci.* **XIV,** 610–611.

Pike, R. J.: 1985, 'Some Morphologic Systematics of Complex Impact Structures, *Meteoritics* **20,** 49–68.

Pike, R. J. and Spudis, P. D.: 1984a, 'Ring Spacing of Mercurian Multi-ring Basins and Basin Ring Formation', *Repts. Planetary Geology Program – 1983*, NASA Tech. Memo. 86246, 90–92.

Pike, R. J. and Spudis, P. D.: 1984b, 'Similar Spacing of Basin Rings on Mars, Mercury, and the Moon', *Lunar Planet. Sci.* **XV,** 647–648.

Pike, R. J., Spudis, P. D., and Clow, G. D.: 1985, 'Average Spacing for Rings of Individual Multi-Ring Basins is $2.0^{0.5}$D', *Repts. Planetary Geology and Geophysics Program – 1984*, NASA Tech. Memo. 87563, 189–191.

Quaide, W. L., Gault, D. E., and Schmidt, R. A.: 1965, 'Gravitative Effects on Lunar Impact Structures', *Annals N.Y. Acad. Sci,* **123,** Art. 2, 563–572.

RAND Corporation: 1955, *A Million Random Digits with 100 000 Normal Deviates*, The Free Press, Glencoe, Ill.

Saunders, R. S., Roth, L. E., Elachi, C., and Schubert, G.: 1978, 'Topographic Confirmation of 500 km Degraded Crater North of Ladon Valles Mars', *Repts. Planetary Geology Program 1977–1978,* NASA TM 79729, 157–159.

Schaber, G. G., Boyce, J. M., and Trask, N. J.: 1977, 'Moon-Mercury: Large Impact Structures, Isostasy and Average Crustal Viscosity', *Phys. Earth Planet. Interiors* **15,** 189–201.

Schultz, P. H.: 1976, *Moon Morphology*, Univ. Texas Press, pp. 7–35, 250–255, 460–466, and 472–499.

Schultz, P. H.: 1979, 'Evolution of Intermediate-age Impact Basins on the Moon', *Conf. Lunar Highlands Crust*, Lunar Planet. Inst. Houston, 141–142.

Schultz, P. H.: 1984, 'Impact Basin Control of Volcanic and Tectonic Processes on Mars', *Lunar Planet. Sci. XV*, 728–729.

Schultz, P. H. and Gault, D. E.: 1986, 'Experimental Evidence for Non-proportional Growth of Large Craters', *Lunar Planet. Sci. XVIII*, 777–778.

Schultz, P. H. and Glicken, H.: 1979, 'Impact Crater and Basin Control of Igneous Processes on Mars', *J. Geophys. Res.* **84,** 8033–8047.

Schultz, P. H. and Merrill, R. B. (eds.): 1981, *Proc. Conf. Multi-ring Basins: Formation and Evolution, Proc. Lunar Planet. Sci.* **12A.**

Schultz, P. H., Schultz, R. A., and Rogers, J.: 1982, 'The Structure and Evolution of Ancient Impact Basins on Mars', *J. Geophys. Res.* **87,** 9803–9820.

Schultz, P. H., Orphal, D., Miller, B., Borden, W. F., and Larson, S. A.: 1981, 'Multi-ring Basin Formation: Possible Clues from Impact Cratering Calculations', in *Multi-ring Basins, Proc. Lunar Planet. Sci.* **12A,** pp. 181–195.

Scott, D. H., McCauley, J. F., and West, M. N.: 1978, *Geologic map of the West side of the Moon*, U.S. Geol. Survey Misc. Inves. Map I-1034, scale 1:5 000 000.

Solomon, S. C. and Head, J. W.: 1980, 'Lunar Mascon Basins: Lava filling, Tectonics and Evolution of the Lithosphere', *Rev. Geophys. Space Phys.* **18,** 107–141.

Spudis, P. D.: 1984, 'Mercury: New Identification of Ancient Multi-ring Basins and Implications for Geologic Evolution, *Repts. Planetary Geology Program – 1983*, NASA Tech. Memo. 86246, 87–89.

Spudis, P. D. and Prosser, J. G.: 1984, *Geologic map of the Michelangelo quadrangle of Mercury*, U.S. Geol. Survey Misc. Inves. Map I–1659, scale 1:5 000 000.

Spudis, P. D. and Strobell, M. E.: 1984, 'New Identification of Ancient Multi-ring Basins on Mercury and Implications for Geologic Evolution', *Lunar Planet. Sci.* **XV**, 814–815.

Spudis, P. D., Hawke, B. R., and Lucey, P.: 'Composition of Orientale Basin Deposits and Implications for the Lunar Basin-forming Process', *Proc. Lunar Planet. Sci. Conf. 15, J. Geophys. Res.* **89**, C197–C210.

Spudis, P. D.: 1986, 'Materials and Formation of the Imbrium Basin', in P. D. Spudis and G. Ryder (eds.), *Workshop on Geology and Petrology of Apollo 15 Landing Site*, LPI Tech. Rept. 86–03, pp. 100–104.

Stam, M., Schultz, P. H., and McGill, G. E.: 1984, 'Martian Impact Basins: Morphology Differences and Tectonic Provinces', *Lunar Planet. Sci.* **XV**, 818–819.

Stuart-Alexander, D. E. and Howard, K. A.: 1970, 'Lunar Maria and Circular Basins – A Review', *Icarus* **12**, 440–456.

Trask, N. J. and Guest, J. E.: 1975, 'Preliminary Geologic Terrain Map of Mercury', *J. Geophys. Res.* **80**, 2461–2477.

Van Dorn, W. G.: 1968, 'Tsunamis on the Moon?', *Nature* **220**, 1102–1107.

Van Dorn, W. G.: 1969, 'Lunar Maria: Structure and Evolution', *Science* **165**, 693–695.

Wilhelms, D. E.: 1973, 'Comparison of Martian and Lunar Multi-ringed Circular Basins', *J. Geophys. Res.* **78**, 4084–4095.

Wilhelms, D. E.: 1980a, 'Irregularities of Lunar Basin Structure', *Repts. Planetary Geology Program 1979–1980*, NASA Tech. Memo. 81776, 25–27.

Wilhelms, D. E.: 1980b, 'Geologic Map of Lunar Ringed Impact Basins (abstract)', *Conf. on Multi-ring Basins*, Lunar Planet. Inst. Contrib. 414, Houston, 115–117.

Wilhelms, D. E.: 1984, 'Moon', Chapter 6 in M. H. Carr (ed.), *The Geology of the Terrestrial Planets*, NASA Spec. Publ. 469, pp. 106–205.

Wilhelms, 1987, *The Geologic History of the Moon*, U.S. Geol. Survey Prof. Paper 1348 (in press).

Wilhelms, D. E. and El-Baz, F.: 1977, *Geologic Map of the East Side of the Moon*, U.S. Geol. Survey Misc. Inv. Ser. Map I–948.

Wilhelms, D. E. and McCauley, J. F.: 1971, *Geologic Map of the Near Side of the Moon*, U.S. Geol. Survey Misc. Inv. Ser. Map I–703.

Wilhelms, D. E., Hodges, C. A., and Pike, R. J.: 1977, 'Nested Crater Model of Lunar Ringed Basins', in D. J. Roddy, R. O. Pepin, and R. B. Merrill (eds), *Impact and Explosion Cratering*, Pergamon, N.Y., pp. 539–562.

Wood, C. A.: 1980, 'Martian Double-ring Basins: New Observations', *Proc. Lunar Planet. Sci. Conf. 11th*, 2221–2241.

Wood, C. A. and Head, J. W.: 1976, 'Comparison of Impact Basins on Mercury, Mars and the Moon', *Proc. Lunar Sci. Conf. 7th*, 3629–3651.